Chapter 2
Broadband Vibration Energy Harvesting Techniques

Lihua Tang, Yaowen Yang, and Chee Kiong Soh

Abstract The continuous reduction in power consumption of wireless sensing electronics has led to immense research interests in vibration energy harvesting techniques for self-powered devices. Currently, most vibration-based energy harvesters are designed as linear resonators that only work efficiently with limited bandwidth near their resonant frequencies. Unfortunately, in the vast majority of practical scenarios, ambient vibrations are frequency-varying or totally random with energy distributed over a wide frequency range. Hence, increasing the bandwidth of vibration energy harvesters has become one of the most critical issues before these harvesters can be widely deployed in practice. This chapter reviews the advances made in the past few years on this issue. The broadband vibration energy harvesting techniques, covering resonant frequency tuning, multimodal energy harvesting, and nonlinear energy harvesting configurations are summarized in detail with regard to their merits and applicability in different circumstances.

2.1 Introduction

Portable devices and wireless sensors are conventionally powered by chemical batteries. The use of batteries not only leads to their costly replacement especially for sensors at inaccessible locations, but also causes pollution to the environment. Besides, batteries also place limitation on the miniaturization of micro- or nano-electromechanical systems. With the advances in integrated circuits, the size and power consumption of current electronics have dramatically decreased. For example, a wireless sensor now can be powered at less than 100 μW. Hence, in the past few years, ambient energy harvesting as power supplies for small-scale

L. Tang • Y. Yang (✉) • C.K. Soh
School of Civil and Environmental Engineering, Nanyang Technological University,
50 Nanyang Avenue, Singapore, Singapore 639798
e-mail: tanglh@ntu.edu.sg; cywyang@ntu.edu.sg; csohck@ntu.edu.sg

N. Elvin and A. Erturk (eds.), *Advances in Energy Harvesting Methods*,
DOI 10.1007/978-1-4614-5705-3_2,

electronics has evoked great research interest from various disciplines, including material science, mechanical, civil, and electrical engineering.

Different energy sources existing in the environment around a system, such as sunlight, wind, and mechanical vibration, can be the options for energy harvesting. Among them, pervasive vibration sources are suitable for small-scale power generation of low-power electronics and thus have attracted more research attention. Current solutions for vibration-to-electricity transduction are mostly accomplished via electrostatic [1, 2], electromagnetic [2, 3], or piezoelectric methods [4, 5]. Various models, including analytical models [2, 6], finite element models ([3, 7]) and equivalent circuit models [8, 9], have been established to investigate the energy harvesting capability of each method. No matter which principle was exploited, most of the previous research work focused on designing a linear vibration resonator, in which the maximum system performance is achieved at its resonant frequency. If the excitation frequency slightly shifts, the performance of the harvester can dramatically decrease. Since the majority of practical vibration sources are present in frequency-varying or random patterns, how to broaden the bandwidth of vibration energy harvesters becomes one of the most challenging issues before their practical deployment.

This chapter presents a review of recent advances in broadband vibration energy harvesting. The state-of-the-art techniques in this field, covering resonant frequency tuning, multimodal energy harvesting, and nonlinear energy harvesting configurations, are summarized in detail with regard to their merits and applicability in different circumstances.

2.2 Resonant Frequency Tuning Techniques

When the excitation frequency is known *a priori*, the geometry and dimensions of a conventional linear harvester can be carefully selected to match its resonant frequency with the excitation frequency. However, when the excitation frequency is unknown or varies in different operational conditions, the harvester with pretuned resonant frequency is unable to achieve optimal power output. Hence, in practice a conventional linear harvester is expected to incorporate a resonance tuning mechanism to increase its functionality. According to Roundy and Zhang [10], the resonance can be tuned "*actively*" or "*passively*". The active mode requires continuous power input for resonance tuning. While in the passive mode, intermittent power is input for tuning and no power is required when frequency matching is completed, that is until the excitation frequency varies again.

Resonance tuning methods can be categorized into mechanical, magnetic, and piezoelectric methods. Furthermore, the tuning process can be implemented manually or in a self-tuning way. Manual tuning is very difficult to implement during operation. A fine self-tuning implementation is expected not only to cover the targeted frequency range but also to be capable of self-detecting the frequency

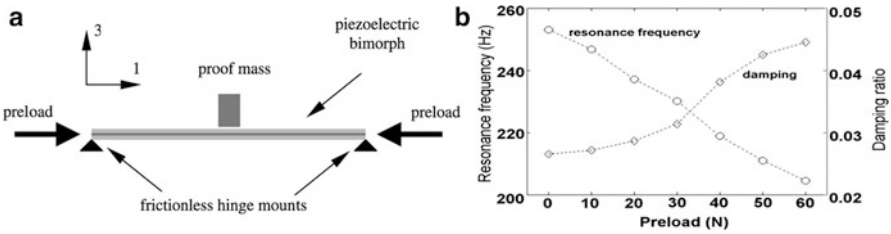

Fig. 2.1 (**a**) Schematic of a simply supported bimorph energy harvester and (**b**) resonance frequency and damping ratio versus tuning preload ([11], copyright: IOP Publishing)

change, automatic control, and of being self-powered consuming as little (harvested energy as possible).

2.2.1 Mechanical Methods

2.2.1.1 Manual Tuning

From elementary of vibration theory, the resonance of a system can be tuned by changing the stiffness or mass. Usually, it is more practical to change the stiffness rather than the mass of the system. Leland and Wright [11], Eichhorn et al. [12], and Hu et al. [13] proposed to apply axial preload to alter the stiffness in their energy harvesting devices, thus tuning the resonant frequencies. In Leland and Wright's work, an axial compressive load was applied on a simply supported bimorph energy harvester (Fig. 2.1a). In their experimental test on the prototype with a 7.1 g proof mass, it was determined that before the bimorph failure, a compressive axial preload can reduce its resonant frequency by up to 24%. Over the frequency range of 200–250 Hz, this protype achieved a power output of 300–400 μW under a 1g excitation acceleration. The power output was relatively flat over this range and even decreased at low frequencies, which could be explained by the increased damping ratio due to the applied preload, as shown in Fig. 2.1b. Besides, the design presented was intended to operate in "passive" mode, where the preload was manually tuned. However, the energy required for the tuning procedure was not addressed. Furthermore, the resonant frequency could only be tuned unidirectionally since only the compressive preload was considered.

Eichhorn et al. [12] presented a cantilever tunable energy harvester by applying prestress at its free end. Figure 2.2a shows the generator and the schematic of the entire setup. The arms connected the tip of the beam and two wings. A revolution of the screw generated compression on the spring, which applied the force on the arms. This force was then applied to the free end of the cantilever through the wings. Below the fracture limit, a resonance shift from 380 to 292 Hz was achieved by applying preload from 7 N to 22.75 N, as shown in Fig. 2.2b. The quality factor

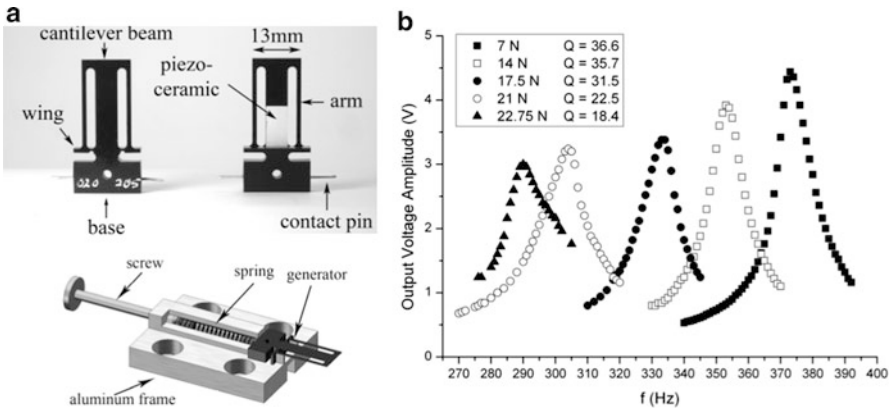

Fig. 2.2 (**a**) Schematic of tunable generator and entire setup and (**b**) resonance curves with various prestresses [12]

was reduced, which means damping arose with increased compression, similar to the finding by Leland and Wright [11].

Analytically, Hu et al. [13] derived the governing equations of a cantilever piezoelectric bimorph with an axial preload and investigated its feasibility and resonance characteristics. The resonance can be adjusted either higher or lower with a tensile or compressive load, respectively. In their model, it was reported that a tensile load of 50 N increased the resonance from 129.3 to 169.4 Hz while the same compressive load decreased the resonance from 129.3 to 58.1 Hz.

Instead of considering the bending mode, some researchers have investigated a tunable resonator working in extensional mode, termed XMR [14, 15]. The XMR presented by Morris et al. [14] was formed by suspending a seismic mass with two piezoelectric membranes (PVDF). Pretensioning two rectangular membranes (with dimensions of $2\,l\times w\times h$ and Young's modulus E) by a rigid link with length of $2u_\mathrm{p}$ and deflecting the link by Δu, as shown in Fig. 2.3a, the force–deflection characteristics of the rigid link were found to be

$$F = \frac{Ewh}{l^3}\left(6u_\mathrm{p}^2\Delta u + 2\Delta u^3\right). \tag{2.1}$$

For sufficiently small deflection, the natural frequency can be approximated as

$$f_\mathrm{N} = \frac{1}{2\pi}\sqrt{\frac{k}{m}} = \frac{1}{2\pi}\sqrt{\frac{\frac{\mathrm{d}F}{\mathrm{d}(\Delta u)}}{m}} \approx u_\mathrm{p}\frac{1}{2\pi}\sqrt{\frac{6Ewh}{ml^3}}. \tag{2.2}$$

Hence, the resonant frequency can be tuned by adjusting the link length that symmetrically pretensions both piezoelectric sheets. Similar force–deflection relationships and natural frequency expressions can be found for other rigidly

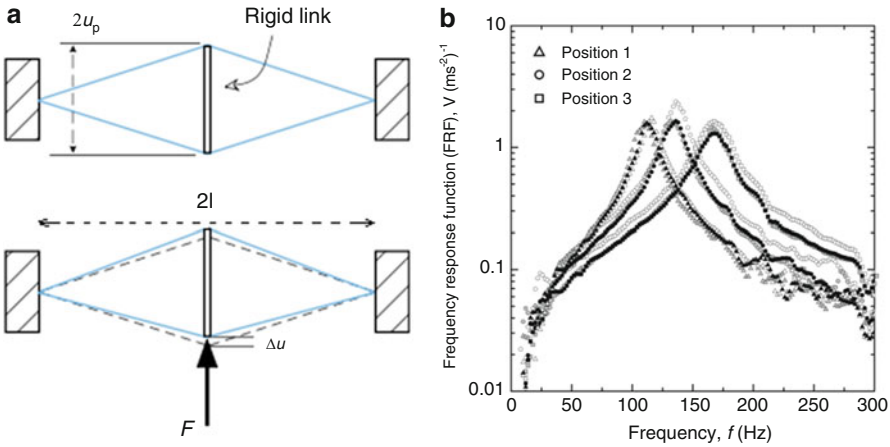

Fig. 2.3 (**a**) Schematic of XMR with two pretensioned membranes by a rigid link and (**b**) frequency responses for three adjustment positions ([14], copyright: IOP Publishing)

coupled and transversely loaded membrane. For the fabricated XMR prototype with a circular configuration, the frequency response functions were obtained by tuning the preloading screw at three random adjustment positions, as shown in Fig. 2.3b. For the developed prototype, it was found that a resonance shift between 80 and 235 Hz can be easily achieved with a change of pretension displacement of around 1.25 mm. Morris et al. [14] claimed that this was not the upper limit of their XMR, which would be constrained by the mechanical failure of the device. However, the capability of self-tuning or sequential tuning during operation of the XMR was not investigated.

A similar investigation was pursued by Loverich et al. [16], in which the resonance can be tuned by adjusting the pre-deflection of the circular plate, as shown in Fig. 2.4. The resonant frequency could be experimentally varied between 56 and 62 Hz by adjusting the boundary location by approximately 0.5 mm. Furthermore, they also made use of nonlinearity of the pre-deflected plate. Similar force–deflection characteristics were obtained as Eq. (2.1). It was found that the stiffness was nearly linear and the system had a high quality factor Q for low vibration amplitudes, while the resonance frequency shifted and Q reduced for high vibration amplitudes. This feature of nonlinear stiffness also provided an auto-protection mechanism, which is important when mechanical robustness is required for high vibration levels.

Rather than applying the axial or in-plane preload, adjusting the gravity center of the tip mass is another idea to adjust the resonance of a cantilever. Wu et al. [17] presented such a device in which the proof mass consisted of a fixed part and a movable part, as shown in Fig. 2.5a. The gravity center of the whole proof mass can be adjusted by driving the movable screw. The mass of the fixed part was much lighter than that of the movable part such that the adjustable distance of the gravity

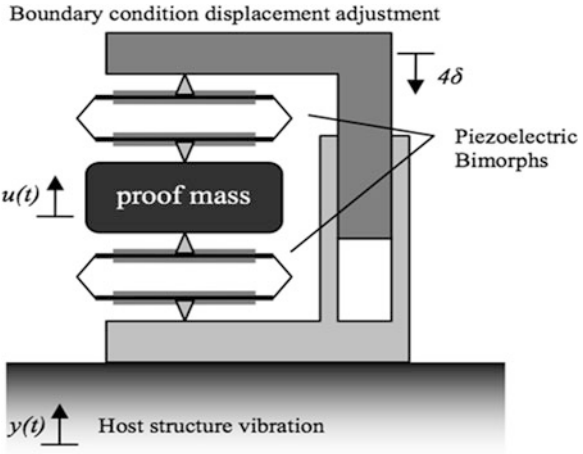

Fig. 2.4 Energy harvester configuration with adjustable boundary condition for inducing large deformation in bimorph plates ([16], copyright: SPIE)

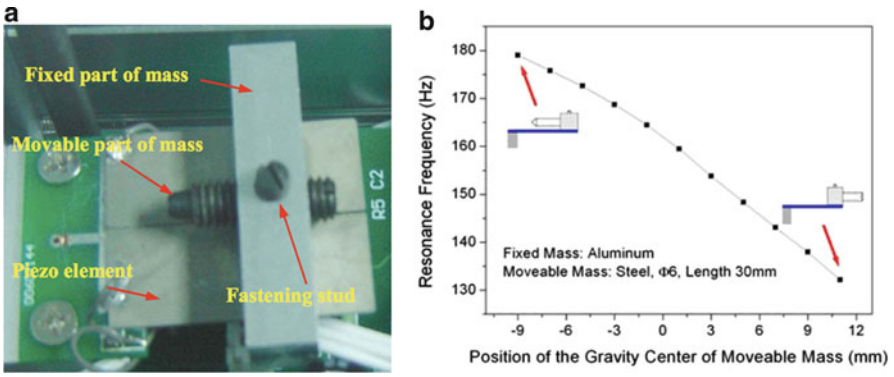

Fig. 2.5 (**a**) Piezoelectric harvester with moveable mass and (**b**) its resonant frequency versus position of gravity center of moveable mass [17]

center of the proof mass and in turn the frequency tunability can be increased. In their prototype, the adjustable resonant frequency range could cover 130–180 Hz by tuning the gravity center of the tip mass up to 21 mm, as illustrated in Fig. 2.5b.

2.2.1.2 Self-Tuning

In Sect. 2.2.1.1, the resonance tuning of the reported devices were implemented manually (usually using screws), which is not favorable for real-time application during operation. To address this problem, some researchers [18, 19] developed novel passive self-tuning harvesters.

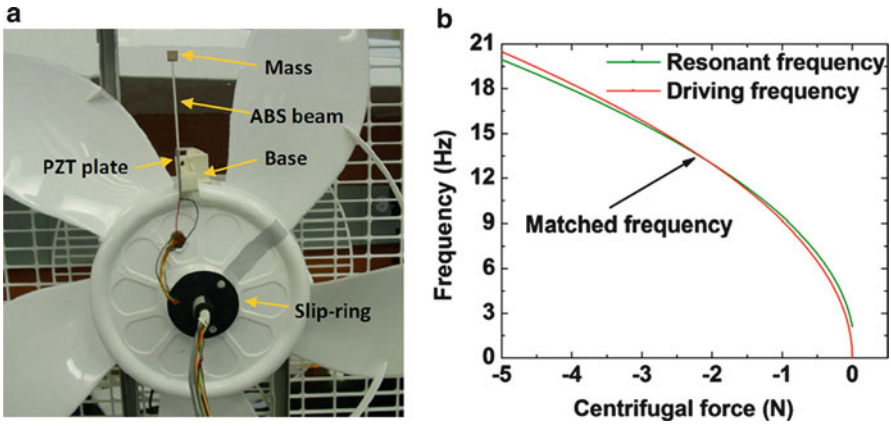

Fig. 2.6 (**a**) Experiment setup for harvesting energy from rotational vibration and (**b**) predicted driving frequency and resonant frequency versus centrifugal force ([18], copyright: American Institute of Physics)

Jo et al. [19] presented a design that was composed of a cantilever couple with different lengths. This cantilever couple was movable laterally and had two operational phases. The horizontal inertia forces exerted to two equal proof masses change with the excitation frequency and become maximum when the excitation frequency matches the resonant frequency. The difference between the horizontal inertia forces is the key to switch the harvester between the two phases. This harvester is self-tunable and no power is required in the tuning procedure. Each cantilever has two resonant peaks as the excitation frequency changes. Although the resonant frequency only switches between two phases and thus can not cover a continuous frequency range, such device is still significantly more efficient than a conventional cantilever harvester without a self-tuning mechanism.

Different from previous research on harvesting energy from translational base excitation, Gu and Livermore [18] focused on rotational motion. A passive self-tuning piezoelectric energy harvester was designed in which centrifugal force was exploited to adjust the stiffness and thus its resonant frequency. The harvester consisted of a radially oriented cantilever beam mounted on a rotational body, as shown in Fig. 2.6a. Since the centrifugal force was related to both driving frequency and resonant frequency of the harvester, the harvester could be designed such that the resonant frequency was exactly equal to the driving frequency at 13.2 Hz. In addition, within a range of 6.2 Hz–16.2 Hz, the two frequencies matched well, as shown in Fig. 2.6b. Thus, the harvester always worked at or near its resonance. In their experiment, the self-tuning harvester could achieve a much wider bandwidth of 8.2 Hz as compared to 0.61 Hz of the untuned harvester. However, this device is only applicable for rotational motion.

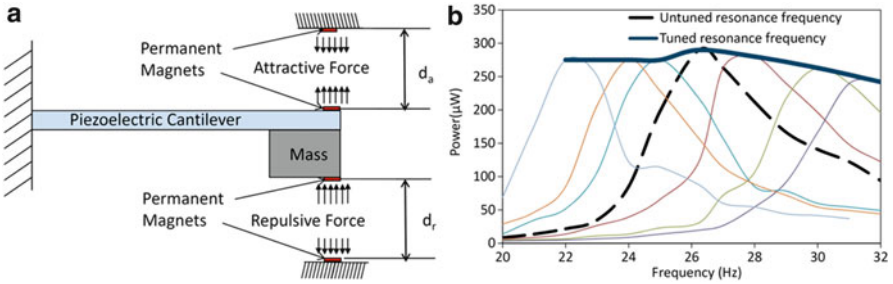

Fig. 2.7 (**a**) Schematic of resonance tunable harvester and (**b**) power output versus tuned resonant frequency in experiment ([20], copyright: IOP Publishing)

2.2.2 Magnetic Methods

2.2.2.1 Manual Tuning

Applying magnetic force to alter the effective stiffness of a harvester is another option for resonance tuning. Challa et al. [20] proposed a tunable cantilever harvester in which two magnets were fixed at the free end of the beam, while the other two magnets were fixed at the top and bottom of the enclosure of the device, as shown in Fig. 2.7a. All magnets were vertically aligned so that attractive and repulsive magnetic forces could be generated on each side of the beam. By tuning the distance between the magnets using a spring-screw mechanism, the prototype with a volume of 50 cm^3 was tunable over the range of 22–32 Hz with a power output of 240–280 μW operating at an acceleration of 0.8 m/s^2. Power output was undermined as the damping increased during the tuning procedure, as shown in Fig. 2.7b. Given the maximum tuning distance of 3 cm, the required energy was estimated to be 85 mJ and it would take 320 s for each tuning procedure. Thus such device can only work where the excitation frequency changes infrequently.

Reissman et al. [21] demonstrated a tuning technique using variable attractive magnetic force, as shown in Fig. 2.8a. The resonance of the piezoelectric energy harvester could be tuned bidirectionally by adjusting a magnetic slider. This is a much simplified design as compared to the design of Challa et al. [20]. The effective stiffness of the piezoelectric beam was dependent on the structural component K_m, the electromechanical component K_e that varied with external resistive loading R_l, and the magnetic stiffness $K_{magnetic}$ that varied with the relative distance D between the two magnets, i.e.,

$$K_{eff} = (K_m + K_e(R_l)) + K_{magnetic}(D). \tag{2.3}$$

By tuning the vertical relative distance D_y of the two magnets, the resonance could be tuned bidirectionally. For a specific D_x, the maximum frequency achieved was 99.38 Hz at $D_y = 0$, and the lowest frequency was 88 Hz at $D_y = 1.5$ cm, as

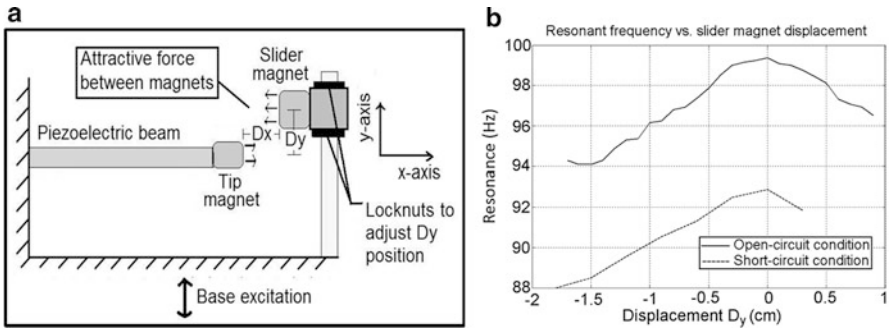

Fig. 2.8 (**a**) Schematic of proposed resonance-tunable harvester and (**b**) open- and short-circuit resonant frequencies with variable D_y ([21], copyright: SPIE)

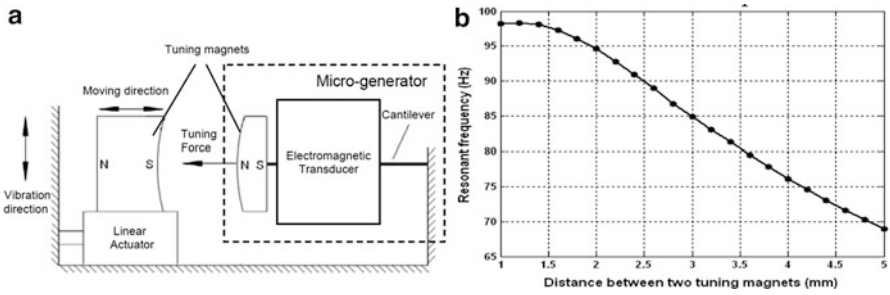

Fig. 2.9 (**a**) Schematic of tuning mechanism and (**b**) resonant frequency versus distance between two magnets [22]

shown in Fig. 2.8b. Hence, the total bandwidth of the harvester was 11.38 Hz, including the resonant frequency shift from short-circuit to open-circuit condition due to the piezoelectric coupling.

In the aforementioned two designs, no "smart" controller for resonance tuning process was implemented.

2.2.2.2 Self-Tuning

Zhu et al. [22] proposed a similar setup as Reissman et al. [21], but they further implemented an automatic controller for resonance tuning. A schematic of the tuning mechanism is shown in Fig. 2.9a. The microcontroller woke up periodically, detected the output voltage of the generator and gave instructions to drive a linear actuator to adjust the distance D between the two magnets. In their experimental test, the resonant frequency was tuned from 67.6 to 98 Hz when D was changed from 5 to 1.2 mm, but it could not be further increased when D was smaller than 1.2 mm, as shown in Fig. 2.9b. At a constant acceleration of 0.588 m/s^2, the power output of 61.6–156.6 μW over the tuning range could be achieved. They

found that the damping of the micro-generator was not affected by the tuning mechanism over most of the tuning range. However, the damping was increased and the output power was less than expected if the tuning force became larger than the inertial force caused by vibration. Additionally, the energy consumed for the tuning procedure in their design was 2.04 mJ mm^{-1}. They claimed that the linear actuator and microcontroller would be ultimately powered by the generator itself to form a closed-loop tuning system. However, experimentally, the tuning system was still powered by a separate power supply for preliminary evaluation. Another drawback was that the control system detected the resonance by comparing the output voltage with a predefined threshold. Thus, such a system could suffer from inefficient detection of the frequency change direction and from mistaken triggering if there was certain change in the excitation amplitude.

Following the work of Zhu et al. [22], Ayala-Garcia et al. [23] presented an improved tunable kinetic energy harvester based on the same tuning mechanism. The phase difference between the harvester and the base was measured in the closed-loop control, which was used to indicate the direction to tune the magnets. A tuning range of 64.1–77.86 Hz (i.e., bandwidth of 13.76 Hz) was achieved by varying the distance between magnets from 5 to 3 mm. However, under the excitation of 0.588 m/s^2, this device required more than 2 h to accumulate enough energy in the supercapacitor of 0.55 F for one tuning process. Challa et al. [24] also improved their previous design [20] by implementing an automatic control system for the tunable harvester. In this improved version, the output power of 736 μW–1 mW was achieved over the tuning range of 13–22 Hz. However, the energy of 3.2–3.9 J was consumed during the tuning process, which required 72–88 min to recover for the next tuning.

Although the above magnetic tuning harvesters implemented automatic control systems, they were not self-powered. Hence, strictly speaking, they have not achieved complete "self-tuning." Besides, the required energy for one tuning procedure is a huge burden in these devices, thus they are only suitable for the vibration scenarios where small and infrequent frequency changes occur. The magnets and control systems also increase the complexity of system design and integration.

2.2.3 Piezoelectric Methods

A piezoelectric transducer used as an actuator can alter the stiffness of a system. In fact, the stiffness of the piezoelectric material itself can be varied with various shunt electrical load. Hence, piezoelectric transducers provide another option for resonance tuning. It should be emphasized that the notion "*piezoelectric methods*" refers to the methods for resonance tuning using piezoelectric transducers. The energy generation method could be electrostatic, electromagnetic, or piezoelectric conversion.

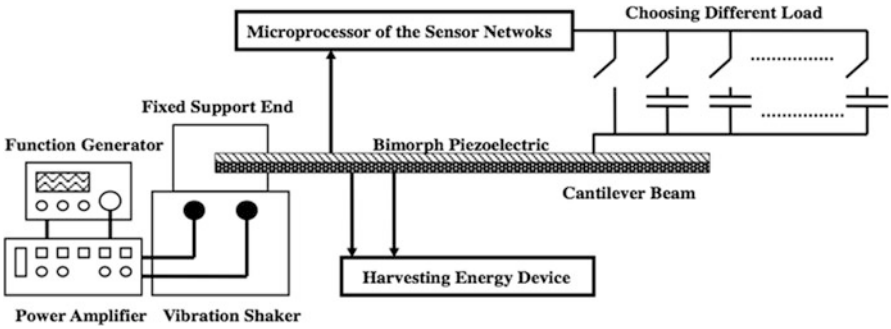

Fig. 2.10 Experiment setup of the tunable energy harvesting system ([25], copyright: SPIE)

Wu et al. [25] presented a piezoelectric bimorph generator in which the upper piezoelectric layer connected to various capacitive loads was used for tuning purpose; the lower layer was used for energy harvesting to charge a supercapacitor, as shown in Fig. 2.10. The tunable bandwidth of the generator was 3 Hz from 91.5 to 94.5 Hz, which was much narrower than achieved by the other aforementioned designs. In the two demo tests, the device was excited under a chirp and random vibration from 80 to 115 Hz, an average harvested power of 1.53 mW and 1.95 mW were generated, respectively, when the real-time tuning system was turned on. These results corresponded to an increase of 13.4% and 27.4% respectively as compared to the output when the tuning system was turned off. A microcontroller was utilized to sample the external frequency and adjusted the capacitive load to match the external vibration frequency in real time, in other words, the device was tuned actively. The continuous power required by the microcontroller system was on μW level.

Peters et al. [26] proposed another novel tunable resonator whose mechanical stiffness and hence the resonance could be adjusted through two piezoelectric actuators. The free actuator swung around the axis of rotation with a deflection angle α, as shown in Fig. 2.11a. By applying a voltage on the actuators, both ends of the actuators were deflected by $\Delta y(V_{\text{op}})$, as shown in Fig. 2.11b. Such deformation caused an additional hinge moment and thus a stiffer structure. One of their fabricated resonators achieved a large tuning of over 30% from an initial frequency of 78 Hz, using a tuning voltage of only ±5 V, as shown in Fig. 2.11c. A discrete control circuit, which exploited the phase characteristic of the resonator, was implemented to actively control the resonance tuning. However, the power consumption of around 150 mW was supplied externally, which significantly outweighed the harvested power (1.4 mW). Thus, the development of a low-power CMOS integration control circuit was recommended for practical closed-loop automatic tuning.

Roundy and Zhang [10] investigated the feasibility of active tuning mechanism. Via an analytical study, they demonstrated that an "active" tuning actuator never resulted in a net increase in power output for the actuator shown in Fig. 2.10. The fabricated piezoelectric generator, with an active tuning actuator is shown

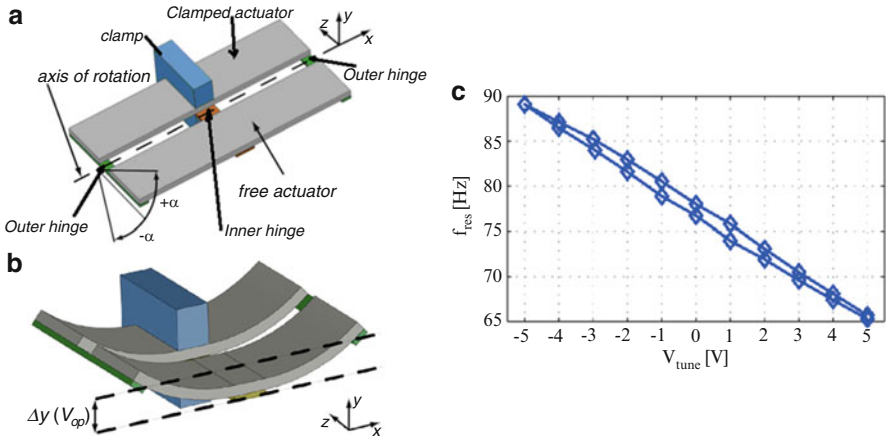

Fig. 2.11 (**a**) Tunable resonator with one clamped and one free actuator; (**b**) Both ends of the actuators are deflected by $\Delta y(V_{op})$ with applied tuning voltage; (**c**) Measured resonance frequency versus applied tuning voltage ([26], copyright: IOP Publishing)

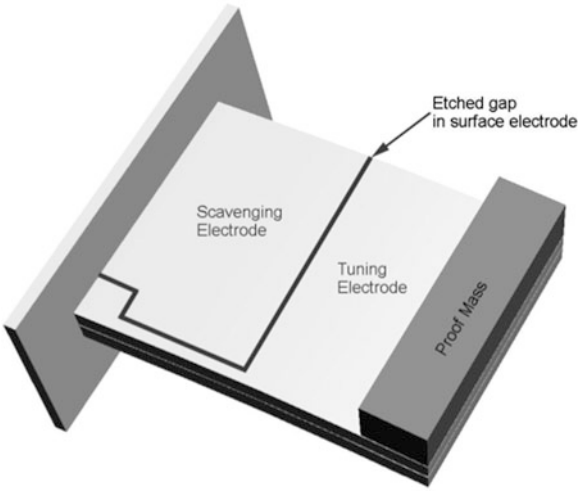

Fig. 2.12 Schematic of a piezoelectric bender, in which the surface electrode is etched to a scavenging and a tuning part ([10], copyright: SPIE)

in Fig. 2.12. The electrode was etched to create a scavenging and a tuning part. Through three experimental test cases, it was found that the change in power output (82 μW) as a result of tuning was significantly smaller than the power needed to continuously drive the actuator (440 μW), which verified the conclusion of their analytical study. They suggested that "passive" tuning mechanism was worth more attention.

Lallart et al. [27] proposed a low-cost self-tuning scheme in which self-detection of frequency change and self-actuation were implemented. The schematic of the system is shown in Fig. 2.13. One layer of the piezoelectric bimorph was used

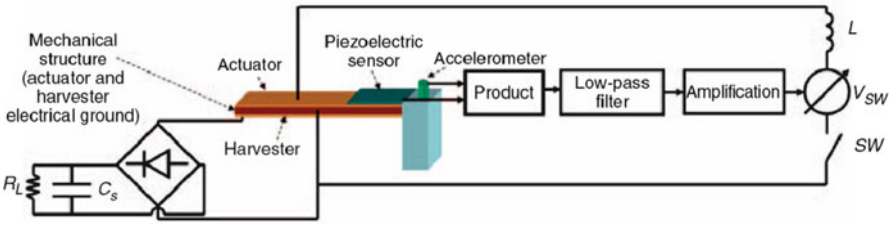

Fig. 2.13 Schematic of self-tuning system ([27], copyright: SAGE Publications)

as harvester and another layer as actuator to tune the stiffness of the structure via an external switching voltage source. An additional piezoelectric sensor and an accelerometer recorded the beam deflection and base acceleration. The self-detection of frequency change was based on the average product of these two signals, which gave the phase information and instructed the closed-loop control to apply the actuation voltage V_S. The most critical part of the required power for tuning in this device was the power for actuation P_{act}. V_S and P_{act} were given by

$$V_S = \pm\beta \frac{\alpha}{C_0} \langle V_{base} \times V_{cant} \rangle \tag{2.4a}$$

$$P_{act} = \frac{\omega}{2\pi} \frac{1+\gamma}{1-\gamma} \frac{\alpha_{act}^2}{(C_0)_{act}} \beta_0^2 \cos(\varphi)^2 u_M^2, \tag{2.4b}$$

where β and β_0 are the user-defined tuning coefficients and φ is the phase between the beam deflection signal V_{cant} and base acceleration signal V_{base}. (Other terms can be found in Lallart et al. [27]). The power needed for actuation is therefore dependent on φ, and can be higher than the harvested power when the excitation frequency is far away from the resonance (Fig. 2.14). The actuation power is zero when the harvester approaches the resonance ($\varphi = \pi/2$). However, frequency detection and information processing modules of the system worked in real time from a continuous external power supply. Thus, this tuning system worked in "active" mode. The proposed system was estimated to achieve a positive net power output and to increase the bandwidth by a factor of 2 (from 4.1 to 8.1 Hz) near the resonance of 112 Hz, as shown in Fig. 2.14. This result is different from the conclusion by Roundy and Zhang [10], in which they could wrongly derive the net power by using the maximum power rather than the average power for actuation [28].

Instead of "active" tuning, Wischke et al. [29] reported a design of a tunable electromagnetic harvester in which the resonance was adjusted in a "semi-passive" way. Figure 2.15a shows the schematic of the design. The maximum tunable frequency range covered 56 Hz between 267 to 323 Hz by applying the voltage −100 V +260 V to the piezoelectric bimorph actuator. This was equivalent to 18% of the basic open-circuit resonant frequency of 299 Hz. More than 50 μW with optimal resistive loading were continuously achieved across the tunable frequency

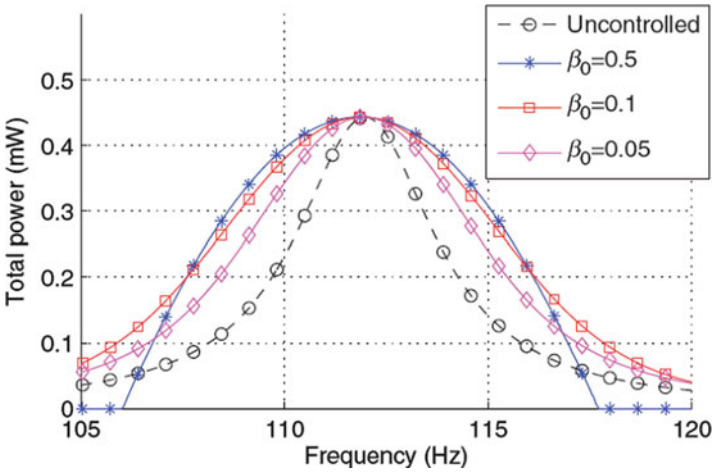

Fig. 2.14 Estimation of net power by proposed technique ([27], copyright: SAGE Publications)

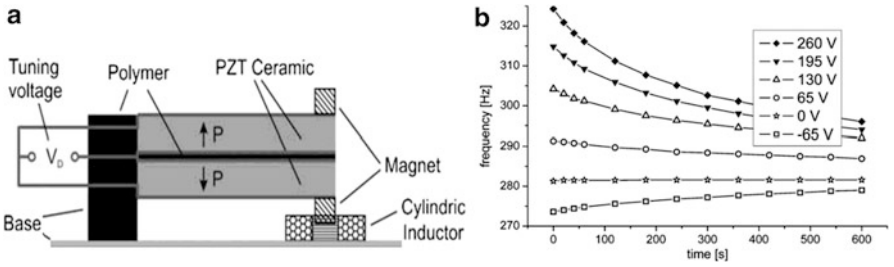

Fig. 2.15 (**a**) Schematic of the device and (**b**) time response of the harvester's operating frequency after the control voltage was disconnected ([29], copyright: IOP Publishing)

range. However, once the control voltage was disconnected, the frequency drifted away from the initial adjusted value due to leakage of the piezoceramic, as shown in Fig. 2.15b. This drift was more intense for high control voltages (>130 V). The charge had to be refreshed periodically to maintain the desired resonant frequency. Hence, the tuning mechanism was defined as "semi-passive" since it is different from the "passive" principle, in which the charge on the piezoceramic and accordingly the adjusted frequency would remain constant after disconnecting the control voltage. In order to reduce the frequency drifting and the energy consumed, the tuning range was suggested to be limited to 25 Hz by applying a voltage of −65 V +130 V, which was still feasible for sensor nodes. To further reduce the energy required for tuning, the shorter electrode of 10 mm length was used, which could achieve 80% of the tuning range, i.e., 20 Hz. Hence, given the power output of 50 μW, 20% circuit efficiency and 200 μJ required for tuning, the resonant frequency of the harvester could be tuned across 20 Hz every 20 s.

2.2.4 Comments on Resonant Frequency Tuning Techniques

Table 2.1 compares the reported resonance tuning methods with regard to tunability (frequency change Δf/average frequency f_{ave}), tuning load, tuning energy required, and whether the harvester is self-tunable.

- *Mechanical methods*. From Table 2.1, generally, mechanical tuning can achieve the largest tunability. However, most of the tunable designs using mechanical method required manual adjustment of the system parameters, such as the preload, pre-deflection, or gravity center of the tip mass. Tuning screws were widely used in these adjusting procedures, which makes it difficult to implement automatically during operation. The mechanical work required for tuning was not addressed in the literature reviewed. Only a few self-tuning mechanical methods [18, 19] enabled the harvesters to be self-adaptive to the vibration environment by exploiting the frequency-dependent inertia force. These devices were capable of automatic tuning during operation without external power input. However, they were applicable for specific conditions. For example, the device by Gu and Livermore [18] only worked for rotational vibration, and the design by Jo et al. [19] only had two working phases (similar to the 2DOF harvesters discussed in Sect. 2.3).
- *Magnetic methods*. Using magnets for resonance tuning can achieve moderate tunability. Automatic control and tuning can be implemented to adjust the distance between the magnets by using linear actuators. Thus, automatic tuning can be achieved during operation. However, the control and tuning systems of reported devices were still powered externally, which means that they were not completely "self-tuning." Moreover, the required energy for tuning was a huge burden in these devices compared to the harvested energy. Thus they are only suitable for the scenarios where small and infrequent frequency changes occur. The use of magnets and control systems also increase the complexity of system design and integration.
- *Piezoelectric methods*. As shown in Table 2.1, piezoelectric methods provide the smallest tunability as compared to the mechanical and magnetic methods. However, since the piezoelectric transducer itself functions as both the controller and tuning component, it is convenient to implement automatic tuning by applying voltage to the transducer or switching the shunt electrical load. In some reported designs [10, 26], the power required for active tuning significantly outweighed the harvested power. However, Wu et al. [25] reported that the required tuning power was only in μW level such that net power increase could be obtained. The reason for this difference is that the concept in Wu et al. [25] was piezoelectric shunt damping where power was only required to continuously switch the shunt electrical load, rather than to apply the voltage to the actuator. The latter usually consumes much more power [27]. Besides, when voltage is applied to the actuator, the leakage of piezoceramic increases the power consumption. Although the shunt damping concept requires small power,

Table 2.1 Summary of reported resonant frequency tuning methods

Author	Methods	Tuning range	Tunability ($\Delta f/f_{ave}$)	Load (force, distance, voltage)	Energy or power for tuning	Manually tuning	Self-tuning		
							Self-detection	Automatic control	Self-powered
Leland and Wright [11]	Mechanical (passive)	200–250 Hz (7.1 g tip mass)	22.22%	Up to 65 N	–	√	–	–	–
Eichhorn et al. [12]	Mechanical (passive)	292–380 Hz	26.19%	Up to 22.75 N	–	√	–	–	–
Hu et al. [13]	Mechanical (passive)	58.1–169.4 Hz	97.85%	−50–50 N	–	√	–	–	–
Morris et al. [14]	Mechanical (passive)	80–235 Hz (can be wider)	≥98.41%	≈1.25 mm	–	√	–	–	–
Loverich et al. [16]	Mechanical (passive)	56–62 Hz	10.17%	0.5 mm	–	√	–	–	–
Wu et al. [17]	Mechanical (passive)	130–180 Hz	32.26%	21 mm	–	√	–	–	–
Jo et al. [19]	Mechanical (passive)	Switch (24 Hz ⟺ 32 Hz)	–	–	–	–	√ (Self-adaptive, no need of external power)		
Gu and Livermore [18]	Mechanical (passive)	6.2–16.2 Hz	89.29%	–	–	–	√ (Self-adaptive, no need of external power)		
Challa et al. [20]	Magnetic (passive)	22–32 Hz	37.04%	3 cm	85 mJ	√	–	–	–

Reissman et al. [21]	Magnetic (passive)	88–99.38 Hz	12.15%	1.5 cm	–	√	–	–	–
Challa et al. [24]	Magnetic (passive)	13–22 Hz	51.43%	10 mm	3.2 J–3.9 J	–	√	√	×
Zhu et al. [22]	Magnetic (passive)	67.6–98 Hz	36.71%	3.8 mm	2.04 mJ mm^{-1}	–	√	√	×
Ayala-Garcia et al. [23]	Magnetic (passive)	64.1 –77.86 Hz	19.39%	2 mm	0.191 J	–	√	√	×
Wu et al. [25]	Piezoelectric (active)	91.5–94.5 Hz	3.23%	–	μW level(controller)	–	√	√	Not mentioned
Peters et al. [26]	Piezoelectric (active)	66–89 Hz(actuator PL140)	29.68%	±5 V	150 mW (discrete controller)	–	√	√	×
Roundy and Zhang [10]	Piezoelectric (active)	64.5–67 Hz	3.80%	5 V	440 μW	–	√	√	×
Lallart et al. [27]	Piezoelectric (active)	8.1 Hz(around resonance of 112 Hz)	7.23%	V_S[Eq. (2.4a)]	P_{act}[Eq. (2.4b)]	–	√	√	×
Wischke et al. [29]	Piezoelectric (semi-passive)	20 Hz (10 mm long electrode)	≈6.7%	−65–+130 V	200 μJ	–	√	√	×

Note: – not applicable, √ implemented, × not implemented

it provides the lowest tunability, as compared to other piezoelectric methods (Table 2.1).

- *Active tuning versus passive tuning*. Active tuning is usually implemented by piezoelectric tuning methods. Generally, it requires more power input than passive tuning, and the tuning power may outweigh the harvested power. However, a net power increase is still possible in active tuning mode if resonance tuning is only required in a very limited range [25, 27]. Passive tuning requires less power input to periodically detect and change the frequency, which is suitable when the excitation frequency varies infrequently. However, if the harvested power can sustain the continuous power required for tuning, an active tuning harvester can work for the excitation with constantly changing frequency or under random excitation, such as the case studied by Wu et al. [25].

2.3 Multimodal Energy Harvesting

In practice, energy harvesters are multiple degree-of-freedom (DOF) systems or distributed parameter systems. Thus one of the vibrational modes of the harvester can be excited when the driving frequency approaches the natural frequency associated with the particular mode. If multiple vibration modes of the harvester are utilized, useful power can be harvested i.e. a wider bandwidth can be covered for efficient energy harvesting. Here, such techniques are termed "multimodal energy harvesting."

Some researchers have reported on theoretical investigations of exploiting the translation and rotation modes of a rigid body [30] or multiple translation modes of lumped parameter systems [31, 32] for multimodal energy harvesting. However, in practice, multimodal energy harvesters are usually implemented by exploiting multiple bending modes of a continuous beam or by an array of cantilevers.

2.3.1 Exploiting Multiple Bending Modes of a Continuous Beam

Roundy et al. [33] first proposed the idea of multiple-DOF system incorporating multiple proof masses attached on a clamped–clamped beam to achieve wider bandwidth. One implementation of this idea was the multifrequency electromagnetic harvester developed by Yang et al. [34]. Other than this work, most of the reported studies in the literature exploited a multimodal harvester with a cantilever beam configuration, in which the first two bending modes were used (in other words, a 2DOF vibration energy harvester).

Tadesse et al. [35] presented a cantilever harvester integrated as part of a hybrid energy harvesting device. The harvester consisted of a cantilever beam with bonded piezoelectric plates and a permanent magnet attached at the tip, which

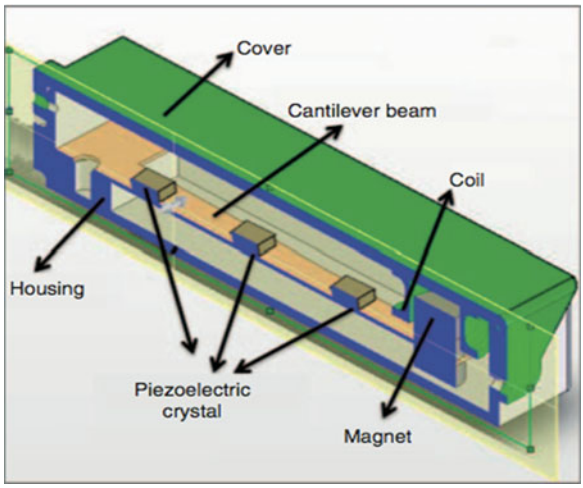

Fig. 2.16 Schematic of the multimodal energy harvesting device ([35], copyright: SAGE Publications)

oscillated within a stationary coil fixed to the housing, as shown in Fig. 2.16. The electromagnetic scheme generated high output power for the first mode, while the piezoelectric scheme was efficient for the second mode. However, the first resonance and the second resonance of such device were far away from each other (20 Hz and 300 Hz). Such discrete effective bandwidth may only be helpful when the vibration source has a rather wide frequency spectrum. The increased size may be another drawback since the permanent magnet is usually difficult to scale down. Besides, a drastic difference of matching loads for electromagnetic and piezoelectric harvesting presents a difficulty in interface circuit design to combine the power outputs from the two schemes.

Ou et al. [36] theoretically modeled a two-mass cantilever beam for broadband energy harvesting. Although two useful modes were obtained, similar to Tadesse et al. [35], they were quite far apart at 26 Hz and 174 Hz, respectively. Arafa et al. [37] presented a similar 2DOF cantilever piezoelectric energy harvester in which one proof mass functioned as a dynamic magnifier (Fig. 2.17a). For the prototype they fabricated, the power output with the dynamic magnifier reached 230 $\mu W/m/s^2$, increasing the power of a conventional harvester without magnifier by a factor of 13.12. Besides, it was observed (see Fig. 2.17b) that the two modes in Fig. 2.17b that the two modes were much closer as compared to those in Ou et al. [36] and Tadesse et al. [35]. However, the magnifier with a spring beam length of 70 mm and a magnifier mass of 11.2 g significantly increases the volume and weight of the original harvester composed of a 52 mm piezoelectric bimorph and a proof mass of 2.06 g.

Erturk et al. [38] exploited an L-shaped cantilever piezoelectric structure for multimodal energy harvesting, as shown in Fig. 2.18a. With proper parameter selection, the second natural frequency was approximately double the first, as shown in Fig. 2.18b. However, how to avoid mode-shape-dependent voltage cancelation was a critical issue. For the three piezoelectric segments combined in series,

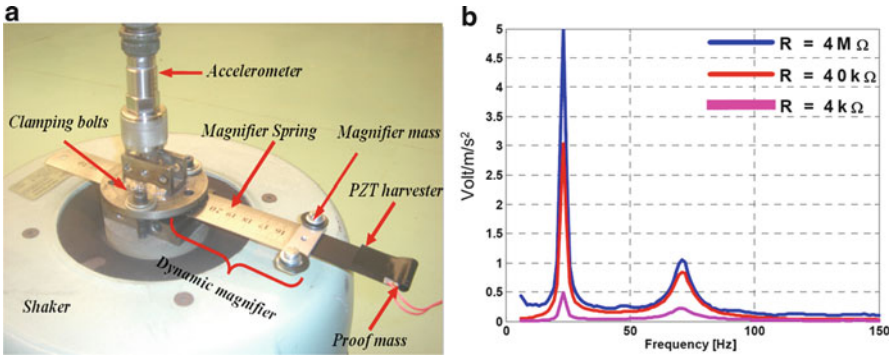

Fig. 2.17 (**a**) Piezoelectric energy harvester with dynamic magnifier and (**b**) its voltage responses of first two modes ([37], copyright: SPIE)

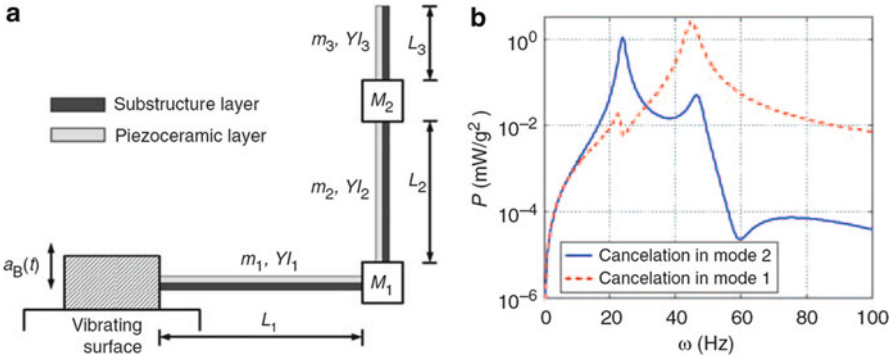

Fig. 2.18 (**a**) Schematic of L-shaped piezoelectric energy harvester. (**b**) Power frequency response function for 50 kΩ load resistance ([38], copyright: SAGE Publications)

cancelation occurred for the second mode. Changing the leads from the first piezoelectric segment in a reverse manner could avoid the cancelation of the second mode but this caused the cancelation for the first mode instead. Thus a more sophisticated interface circuit is required to adaptively change the electrode leads or to deliver the energy separately to avoid voltage cancelation.

Berdy et al. [39] reported a wide-band vibration energy harvester composed of a cantilevered symmetric meandering bimorph and a distributed proof mass. The concept of this design is shown in Fig. 2.19. The fabricated prototype successfully achieved two closely spaced resonant modes at 33 Hz and 43.3 Hz with measured RMS output powers of 107.3 μW and 74.9 μW, respectively, at a peak acceleration of $0.2 \times g$. In a wide bandwidth of 32.3–45 Hz, the output power remained above 25 μW. Another advantage of this device was that the sensing electronics and circuit board could be used as the distributed proof mass thus achieving a compact system.

Wu et al. [40] developed a novel compact 2DOF energy harvester, as shown in Fig. 2.20a. This device was fabricated from the conventional SDOF harvester by

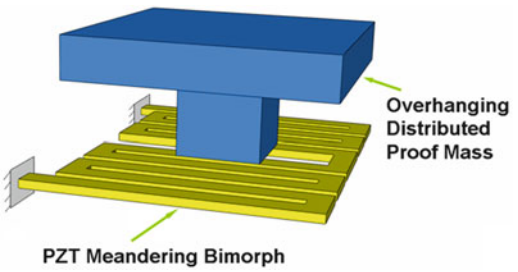

Fig. 2.19 Concept of meandering energy harvester with distributed proof mass

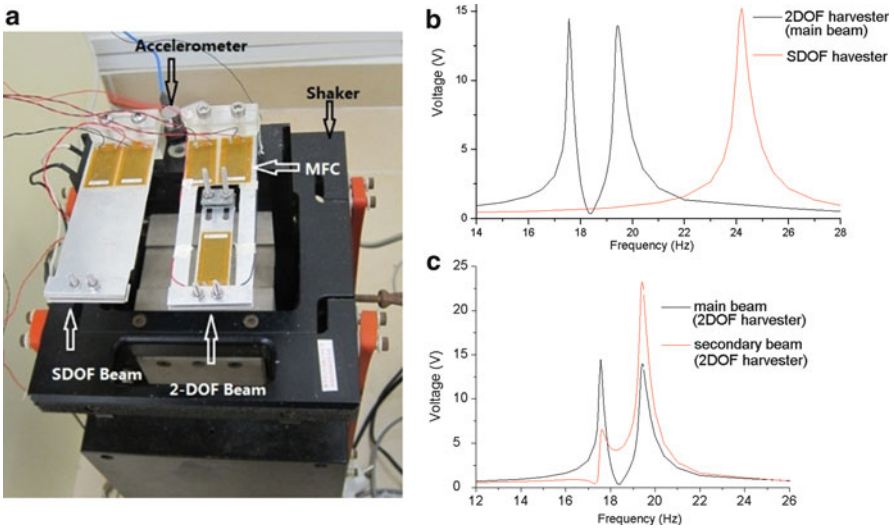

Fig. 2.20 (**a**) Conventional SDOF (proof mass $M_1 = 7.2$ g) and proposed 2DOF harvesters (proof mass $M_1 = 7.2$ g on main beam and $M_2 = 11.2$ g on secondary beam) installed on seismic shaker. (**b**) Comparison of open-circuit voltages from conventional SDOF and proposed 2DOF harvester. (**c**) Comparison of open-circuit voltages from main beam and secondary beam of proposed 2DOF harvester [40]

cutting out a secondary beam inside the main beam. Compared to the conventional SDOF harvester, this device was able to generate two close effective peaks in voltage response with properly selected parameters, as shown in Fig. 2.20b. Thus, multimodal energy harvesting was achieved with only a slight increase of the system volume. Besides, significant voltage output could be obtained from the secondary beam (Fig. 2.20c), which was not utilized due to the low strain level in the conventional SDOF configuration. Thus, this device efficiently utilized the material of the cantilever beam. Moreover, as compared to previously reported 2DOF harvester designs, it was more compact and could have two resonant frequencies much closer to each other.

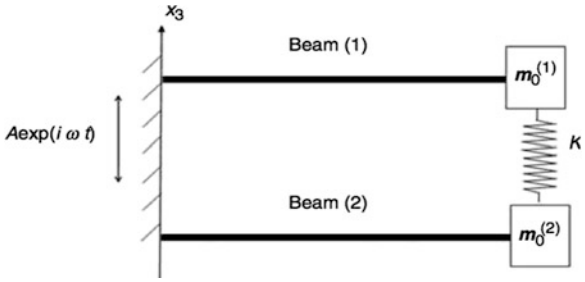

Fig. 2.21 Schematic of two beams with two end masses elastically connected ([41], copyright: SAGE Publications)

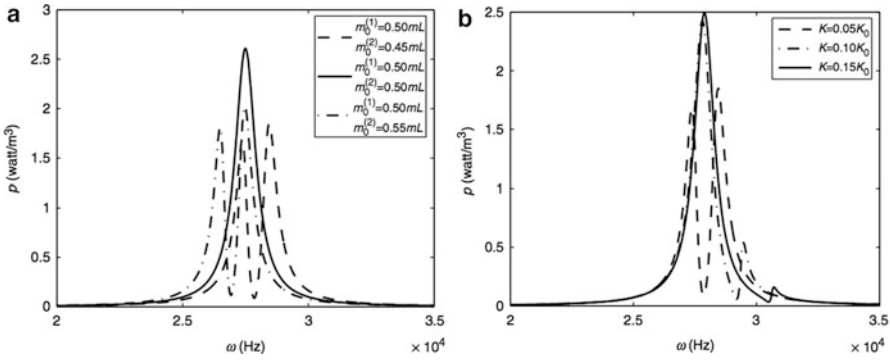

Fig. 2.22 Power density versus frequency for (**a**) different end mass pairs with a fixed spring stiffness and (**b**) different spring stiffness with a fixed mass pair ($m_0^{(1)} \neq m_0^{(2)}$) ([41], copyright: SAGE Publications)

2.3.2 Cantilever Array Configuration

Different from the discrete bandwidth corresponding to the multiple modes of a single beam, multiple cantilevers or cantilever arrays integrated in one energy harvesting device can easily achieve continuous wide bandwidth if the geometric parameters of the harvester are appropriately selected. Similar to the configurations in Sect. 2.3.1, sophisticated interface circuits are required to avoid charge cancelation due to the phase difference between the cantilevers in array configurations.

Yang and Yang [41] suggested using connected or coupled bimorph cantilever beams for energy harvesting, whose resonant frequencies could be tuned to be very close to each other. Figure 2.21 shows the schematic of the design, and Fig. 2.22 shows the theoretical prediction of power output versus frequency. Similar to Wu et al. [40], two close modes and thus wider bandwidth could be achieved as compared to a single-beam harvester. The amplitude and location of the resonances were found to be sensitive to the end spring and end masses.

Kim et al. [42] developed a 2DOF harvester composed of two piezoelectric cantilevers connected by a common proof mass, as shown in Fig. 2.23a. Although

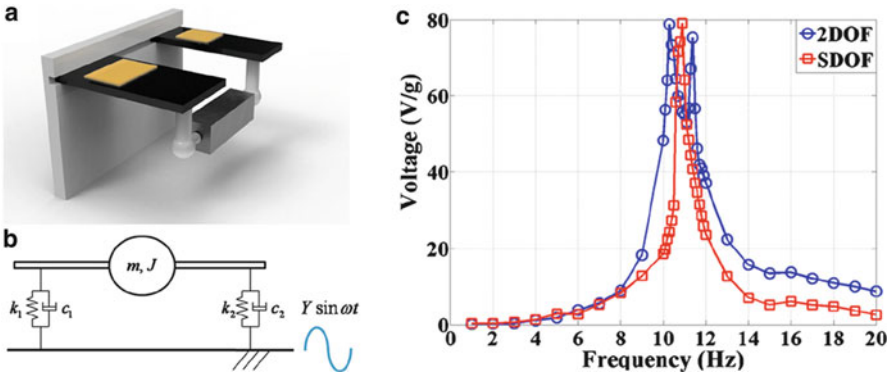

Fig. 2.23 (**a**) Schematic view of proposed device; (**b**) simplified mechanical model; (**c**) Frequency response comparison between proposed 2DOF and SDOF harvesters ([42], copyright: American Institute of Physics)

this design is categorized as a cantilever array configuration in this chapter, it should be emphasized that the underlying principle is to exploit the translational and rotational DOFs of the rigid mass (Fig. 2.23b). The two modes could be designed to be very close to each other and 280% increase in bandwidth at a voltage level of 55 V/g was achieved from a single piezoelectric cantilever in the 2DOF harvester, as compared to a conventional SDOF device in their experiment (Fig. 2.23c).

Other than these previous two designs of two coupled cantilevers, most of the research attempts were made to develop multimodal devices with more cantilevers to tailor and cover desired bandwidth for specific applications [43–47]. Different from Yang and Yang [41] and Kim et al. [42], these cantilevers were usually quasi-uncoupled. Each cantilever was regarded as one substructure of the harvester and thus the first mode of each cantilever was one of the vibration modes of the harvester.

Shahruz [43] designed an energy harvester that consists of piezoelectric cantilevers of various lengths and tip masses attached to a common base (Fig. 2.24a). It was capable of resonating at various frequencies by properly selecting the length and tip mass of each beam and thus provided voltage response over a wide frequency range (Fig. 2.24b). Such combination of cantilevers into a single device created a so-called “mechanical band-pass filter.”

Xue et al. [44] presented a similar design of a broadband energy harvester using multiple piezoelectric bimorphs (PB) with different thickness of piezoelectric layers. They found that the bandwidth of their PB array configuration could be tailored by choosing an appropriate connection pattern (mixed series and parallel connections). Connecting multiple bimorphs in series could broaden the bandwidth. Comparing the single bimorph harvester and a 10-bimorph array configuration, their numerical results showed that not only the power magnitude of the energy harvesting system was increased but also the bandwidth (output power >10 μW) was widened from (97,103)Hz to (87,115)Hz. Furthermore, the bandwidth could be shifted to the dominant frequency range by changing the number of bimorphs in

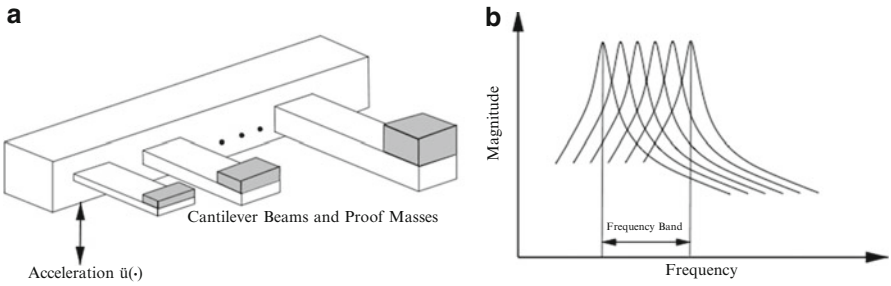

Fig. 2.24 (**a**) Mechanical band-pass filter and (**b**) its transfer function ([43], copyright: Elsevier)

parallel. This shift was due to the change in the electrical boundary condition when increasing or decreasing bimorphs in parallel.

Ferrari et al. [45] developed another multifrequency converter and investigated its feasibility and efficiency for powering a wireless sensor. This device consisted of three piezoelectric bimorph cantilevers with the same dimensions of 15 mm × 1.5 mm × 0.6 mm but with different tip masses ($m_1 = 1.4$ g, $m_2 = 0.7$ g, $m_3 = 0.6$ g). When excited by mechanical vibrations, the device charged the storage capacitor and regularly delivered the energy to the wireless sensor and measurement transmission module. Under resonant excitation, i.e., at either f_1, f_2, or f_3, the corresponding single cantilever in the array could alone trigger the transmission, but a single cantilever could not do so at off-resonance frequency f_4. Conversely, with the complete converter array, the converted energy was high enough to trigger the transmission for all the tested frequency, including f_4. Besides, the shorter switching time (two measure-and-transmit operations) was obtained using the converter array rather than a single cantilever. It was claimed that the wider bandwidth and improved performance were worth the modest increase in size of the proposed array device.

Broadband energy harvesters with cantilever array were also implemented compatibly with current standard MEMS fabrication techniques [46, 47]. Liu et al. [46] implemented such a MEMS-based broadband cantilever array harvester, as shown in Fig. 2.25a. In their experimental test, a phase difference in voltage output from each cantilever was observed, which impaired the voltage output of this three cantilever device (Fig. 2.25b). Thus, the DC voltage across the capacitor after rectification was only 2.51 V, and the maximum DC power output was about 3.15 μW. To address this problem, separate rectifier for each cantilever was required, which increased the total DC voltage to 3.93 V and the maximum DC power output to 3.98 μW. With the wider bandwidth 226–234 Hz and the improved output, such a device was claimed to be promising in applications of ultra-low-power wireless sensor networks. However, the more complicated rectification circuit may cause significant energy loss in these MEMS-scale devices especially for low-level or *off-resonance* excitations. Low-voltage-drop rectification techniques using "active diode" may alleviate this problem in such cases [48].

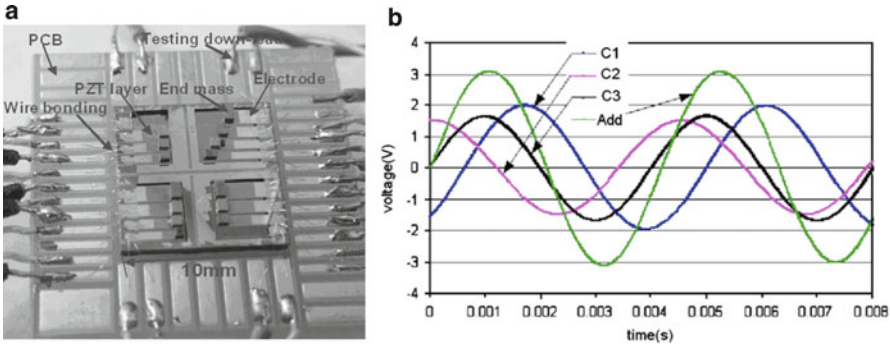

Fig. 2.25 (**a**) Schematic of generator array prototype and (**b**) AC output of three cantilevers in an array and their direct serial connection ([46], copyright: Elsevier)

Sari et al. [47] implemented a micro broadband energy harvester using electromagnetic induction. The developed device generated power via the relative motion between a magnet and coils fabricated on 35 serially connected cantilevers with different lengths. It was reported that 0.4 μW continuous power with 10 mV voltage was generated, covering a wide external vibration frequency range of 4.2–5 kHz. The test was carried out at an acceleration level of $50 \times g$, which was much higher than the $0.5 \times g$ in the test of Liu et al. [46]. The cantilever size had a very similar scale but the power output from the device by Sari et al. [47] was much less than that from the device by Liu et al. [46], which indicated that the piezoelectric conversion was more favorable for vibration energy harvesting on the MEMS scale. Furthermore, the voltage level of 10 mV from the harvester by Sari et al. [47] was more challenging for AC–DC rectification and energy storage.

2.3.3 Comments on Multimodal Energy Harvesting

Multimodal energy harvesting can be implemented by exploiting multiple bending modes of a continuous beam or by exploiting a cantilever array integrated in one device where the first mode of each cantilever is one of the vibration modes of the device. Compared with the resonance tuning techniques, multimodal energy harvesting does not require tuning and hence is much easier to implement. The concerns for multimodal energy harvesting include:

- *Bandwidth*. The multiple bending modes of a continuous beam are usually far away from one another and thus the effective bandwidth is discrete. Some novel structures like L-shaped beams [38], cut-out beams [40], and cantilevered meandering beams [39] can be considered to achieve close and effective resonant peaks. However, in general, only the first two modes can contribute to effective multimodal energy harvesting. By using cantilever arrays, the targeted bandwidth

can be covered continuously by proper selection of the system parameters (see Fig. 2.24b).

- *Power density*. Multimodal energy harvesting increases the bandwidth but is however accompanied by an increased volume or weight of the device. Thus the overall power density (power/volume or power/weight) may be sacrificed. For example, in the cantilever array configuration, only one cantilever or a subset of the array is active and effective for energy generating while the other cantilevers are at an *off-resonance* status. Hence, with the known dominant spectrum of the ambient vibration, the harvester should be carefully designed with a proper number and dimensions of the cantilevers such that the device can cover the targeted bandwidth with the least sacrifice of power density.
- *Complex interface circuit*. Multimodal energy harvesting requires more complex interface circuit than that for a single-mode harvester. A critical electrical issue is to avoid mode shape dependent voltage cancelation in a continuous beam or the cancelation due to the phase difference between cantilevers in array configurations. More sophisticated interface circuits are required to adaptively change the electrode leads or to deliver the energy separately (i.e., each piezoelectric segment in a continuous beam or each cantilever in a cantilever array configuration is connected to a separate load or rectifier). An interface circuit is also required to address the drastic difference in matching load for different energy transduction mechanisms in the hybrid energy harvesting scheme based on a continuous beam [35].

2.4 Nonlinear Energy Harvesting Configurations

In Sect. 2.2 we presented several resonance tuning techniques using magnets [20–22]. Actually these magnets introduce not only a change in the linear stiffness but also a change in the nonlinear stiffness. The nonlinear behavior becomes apparent when the harvester experiences oscillation with significant amplitude. Such nonlinearity also benefits wideband energy harvesting.

As reported in the available literature, nonlinearities in energy harvesters are considered from two perspectives, i.e., nonlinear stiffness [49–57] and nonlinear piezoelectric coupling [58, 59]. Compared to the nonlinear piezoelectric coupling, which results from the manufacturing process of piezoelectric materials, the nonlinear stiffness of a harvester is relatively easier to achieve and control. This section reviews recent advances in designing broadband energy harvesters with nonlinear stiffness.

The dynamics of a general oscillator can be described as

$$\ddot{x} = -\frac{\mathrm{d}U(x)}{\mathrm{d}x} - \gamma\dot{x} + f(t), \tag{2.5}$$

where x represents the oscillator position; γ represents the viscous damping; $f(t)$ is the ambient vibration force; and $U(x)$ is the potential function. If an electromagnetic

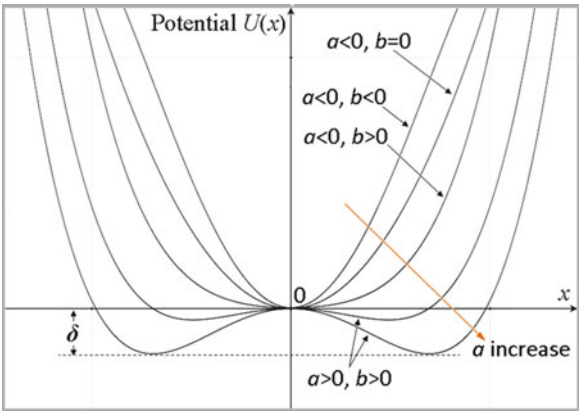

Fig. 2.26 Potential function for different Duffing oscillators

generator is considered, γ includes the viscous damping caused by electromagnetic coupling. Details on this kind of electrical viscous damping can be found in El-Hami et al. [3] or Mann and Sims [50]. For a piezoelectric generator, the damping caused by piezoelectricity cannot be modeled as a viscous damper [60] and Eq. (2.5) should be modified by adding a coupling term as

$$\ddot{x} = -\frac{\mathrm{d}U(x)}{\mathrm{d}x} - \gamma\dot{x} + \kappa V + f(t), \tag{2.6}$$

where κ represents the electromechanical coupling coefficient and V is the voltage on the electrical load. The circuit equations for the piezoelectric and the electromagnetic harvesters are quite different due to differences in their internal impedances. They are not given here but they can be readily found in the literature related to electromagnetic and piezoelectric transductions, such as El-Hami et al. [3] and Erturk et al. [53].

Duffing-type nonlinear oscillator

For a Duffing-type oscillator, the potential energy function $U(x)$ can be considered in a quadratic form as [61, 62],

$$U(x) = -\frac{1}{2}ax^2 + \frac{1}{4}bx^4. \tag{2.7}$$

Thus the Duffing-type oscillator has the cubic nonlinear spring force as

$$F(x) = -ax + bx^3. \tag{2.8}$$

The potential function $U(x)$ for different Duffing oscillators is shown in Fig. 2.26. $U(x)$ is symmetric and bistable for $a > 0$ and $b > 0$ and monostable for $a \leq 0$. In the bistable case, two minima at $x_m = \pm\sqrt{a/b}$ are separated by a barrier δ at $x = 0$.

Piecewise-linear oscillator

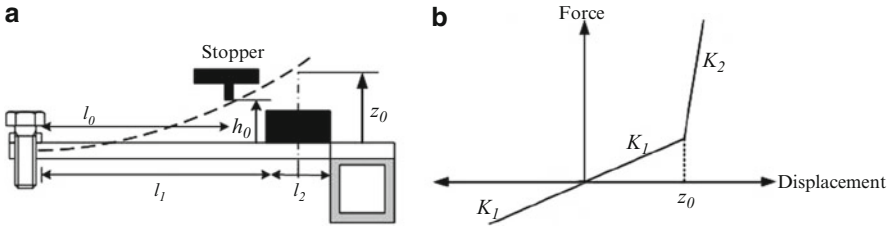

Fig. 2.27 (**a**) Typical mechanical stopper configuration in vibration energy harvester and (**b**) its piecewise-linear stiffness ([63], copyright: IOP Publishing)

Other than the Duffing-type oscillator, some researchers also attempted to exploit piecewise-linear stiffness to increase the bandwidth of vibration energy harvesters. Using mechanical stoppers is one common way to introduce the piecewise-linear stiffness [56, 63–65]. A typical setup of a vibration energy harvester with a mechanical stopper and its nonlinear stiffness are illustrated in Fig. 2.27.

This section reviews both Duffing-type nonlinear harvesters and harvesters with mechanical stoppers. Their benefits on improving the performance of vibration energy harvester are discussed in the following parts.

2.4.1 Monostable Nonlinear Configuration

Substituting Eq. (2.7) into Eq. (2.5) gives the forced Duffing's equation [49, 50, 66],

$$\ddot{x} + \gamma\dot{x} - ax + bx^3 = f(t). \tag{2.9}$$

For $a \leq 0$, it can be used to describe a monostable system. $b > 0$ determines a hardening response, while $b < 0$ a softening response.

Ramlan et al. [49] investigated the hardening mechanism of the nonlinear monostable harvester. Their numerical and analytical studies showed that ideally, the maximum amount of power harvested by a system with a hardening stiffness was the same as the maximum power harvested by a linear system, regardless of the degree of nonlinearity. However, this might occur at a different frequency depending on the degree of nonlinearity, as shown in Fig. 2.28. Such a device has a larger bandwidth over which the significant power can be harvested due to the shift in the resonant frequency.

Mann and Sims [50] presented a design for electromagnetic energy harvesting from nonlinear oscillations due to magnetic levitation. Figure 2.29a shows the schematic of the system where two outer magnets are oriented to repel the center magnet, thus suspending it with a nonlinear restoring force. The derived governing equation has the same form as Eq. (2.9). Figure 2.29b,c shows the experimental velocity response and theoretical predictions under low and high harmonic base

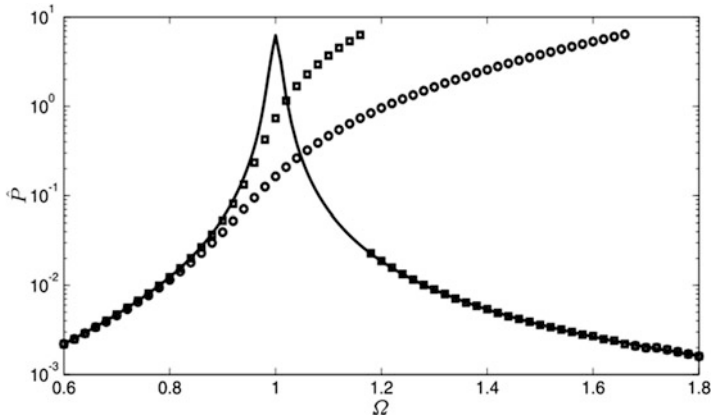

Fig. 2.28 Numerical solution for nondimensional power harvested with damping ratio $\zeta = 0.01$ and excitation amplitude $Y = 0.5$: Linear system (*solid line*), hardening system with nonlinearity $b = 0.001$ (*open square*) and $b = 0.01$ (*open circle*) [b is the coefficient of the nonlinear term in Eq. (2.9)] ([49], copyright: Springer Science+Business Media)

excitation levels, respectively. At low excitation level, the frequency response (Fig. 2.29b) was similar to the response of a linear system. However, at high excitation level, the response curve was bent to the right (Fig. 2.29c). Thus, relatively large amplitudes persisted over a much wider frequency range. Both experiment and theoretical analysis captured the jump phenomena near the primary resonance and the multiple periodic attractors, as shown in Fig. 2.29c. However, such a hardening device only broadened the frequency response in one direction (the peak response shifts to the right).

Stanton et al. [51] proposed another monostable device for energy harvesting using the piezoelectric effect. The device consisted of a piezoelectric beam with a magnetic end mass interacting with the fields of oppositely poled stationary magnets, as shown in Fig. 2.30. The system was modeled by an electromechanically coupled Duffing's equation similar to Eq. (2.9), except that the piezoelectric coupling term κV should be added as in Eq. (2.6). By tuning the nonlinear magnetic interactions around the end mass (i.e., tuning the distance d), both hardening and softening responses may occur, as shown in Fig. 2.31, which allows the frequency response to be broadened bidirectionally. In the experimental validation, a linearly decreasing frequency sweep was performed for the softening case. Different from Ramlan et al. [49], it was shown that not only a wider bandwidth but also a better performance could be obtained by the monostable configuration, as compared to the linear configuration (with stationary magnets removed), as shown in Fig. 2.32. This might be due to the change of damping due to the magnets used in the experiment [20, 22], while a constant damping was used in the analysis by Ramlan et al. [49].

Previous monostable designs have a larger bandwidth due to the shift in the resonant frequency. This nonlinear advantage if the high-energy attractor regime

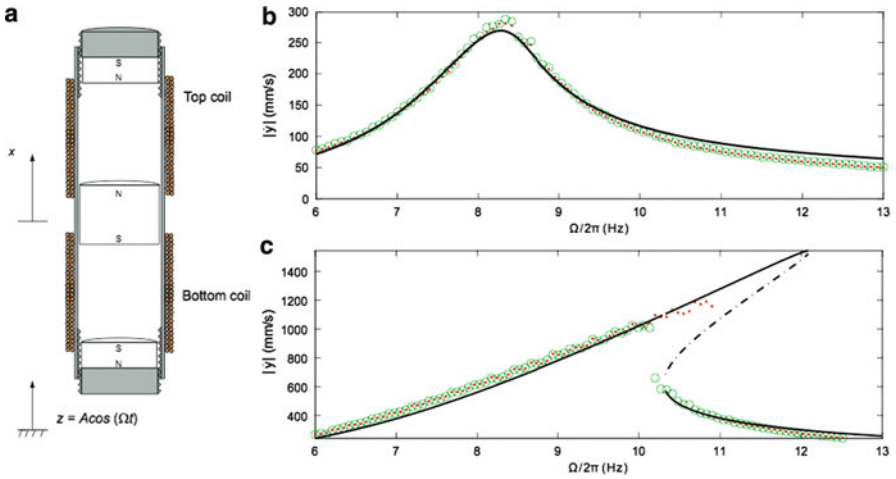

Fig. 2.29 (**a**) Schematic of the magnetic levitation system; experimental velocity response; and theoretical predictions from forward (*red dots*) and reverse (*green circles*) frequency sweep under two excitation levels: (**b**) 2.1 m/s^2 and (**c**) 8.4 m/s^2. Theoretical predictions include stable solutions (*solid line*) and unstable solutions (*dashed line*) ([50], copyright: Elsevier)

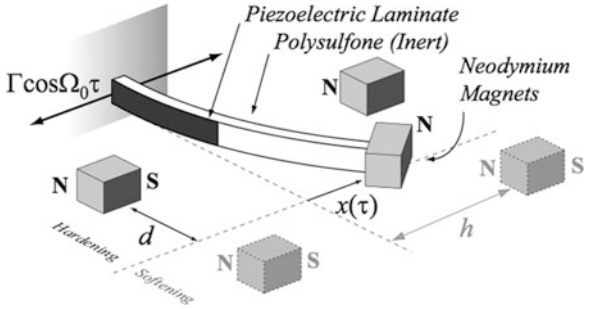

Fig. 2.30 Schematic of proposed nonlinear energy harvester ([51], copyright: American Institute of Physics)

is realized [51]. A linearly decreasing or increasing frequency sweep can capture the high-energy attractor and hence improve the bandwidth for the softening and hardening cases. Unfortunately, such conditions cannot be guaranteed in practice. Certain means of mechanical or electrical disturbance or perturbation is required once the nonlinear devices enter low-energy orbits; otherwise little power can be harvested. Previous reported studies did not address the required momentary perturbation if the harvester is in the low-energy branch and the requisite actuation energy. Furthermore, under a White Gaussian excitation, Daqaq [67] demonstrated that the hardening-type nonlinearity failed to provide any enhancement of output power over typical linear harvesters. Under colored Gaussian excitations, the expected output power even decreased with a hardening-type nonlinearity. This suggested that the monostable configuration may be only applicable for frequency sweep excitations.

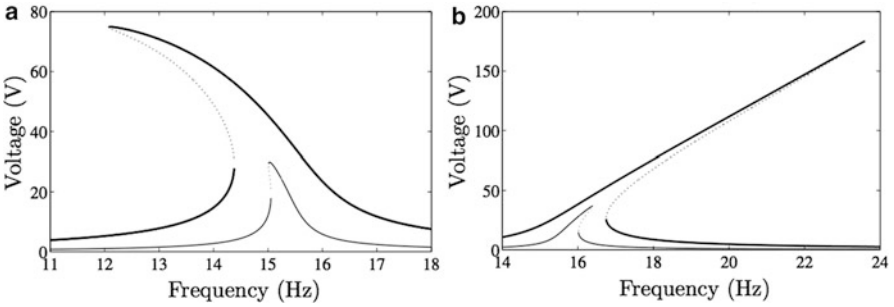

Fig. 2.31 Predicted response amplitudes of output voltage for (**a**) $d = 5$ mm and (**b**) $d = -2$ mm, corresponding to softening and hardening cases, respectively. *Solid lines* correspond to stable solutions while the dotted line to unstable solutions. The *lighter line* and *darker line* correspond to low- and high excitation levels, respectively ([51], copyright: American Institute of Physics)

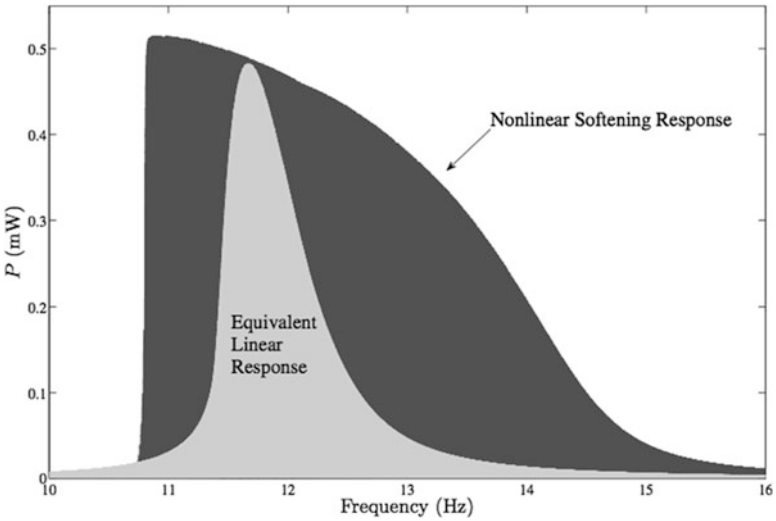

Fig. 2.32 Comparison of energy harvesting performances of nonlinear and linear configurations under the same excitation amplitude of $0.3 \times g$ ([51], copyright: American Institute of Physics)

2.4.2 *Bistable Nonlinear Configuration*

For $a > 0$, Eq. (2.9) can be used to describe a bistable nonlinear system. In this section, we discuss in detail how to exploit the properties of the nonlinearity of a bistable system to improve energy harvesting performance over a wide range of ambient vibration frequencies, subjected to either periodic forcing or stochastic forcing.

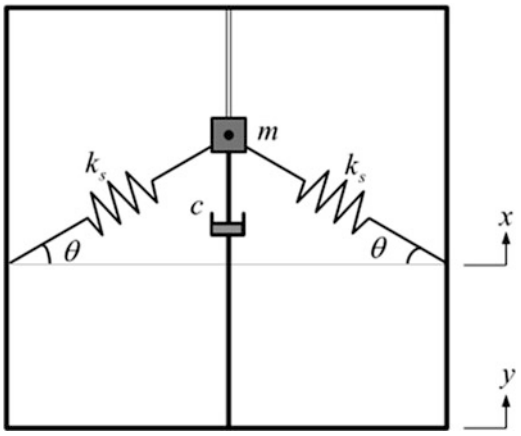

Fig. 2.33 Arrangement of mass-spring-damper generator for the *snap-through* mechanism ([49], copyright: Springer Science+Business Media)

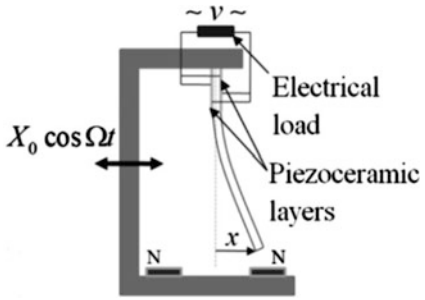

Fig. 2.34 The piezomagnetoelastic generator ([53], copyright: American Institute of Physics)

2.4.2.1 Periodic Forcing

A periodically forced oscillator can undergo various types of large-amplitude oscillations, including chaotic oscillation, large-amplitude periodic oscillation, and large-amplitude quasiperiodic oscillation. The behavior depends on the design of the device, the frequency, and amplitude of the forcing and the damping [66]. One physically realizable energy harvester with bistable nonlinear stiffness was proposed by Ramlan et al. [49], utilizing a so called "*snap-through*" mechanism. The setup consisted of two linear oblique springs connected to a mass and a damper, as shown in Fig. 2.33, yielding a nonlinear restoring force in the x direction. This mechanism has the effect of steepening the displacement response of the mass as a function of time, resulting in a higher velocity for a given input excitation. Numerical results revealed that this mechanism could provide much better performance than the linear mechanism when the excitation frequency was much less than the natural frequency.

Bistable nonlinear stiffness can also be created by using magnets. Erturk et al. [53] and Erturk and Inman [68] pursued such method in designing a broadband piezomagnetoelastic generator. The device consisted of a ferromagnetic cantilever beam with two piezoceramic layers attached at the root for energy generation and with two permanent magnets near the free end, as illustrated in Fig. 2.34. For an

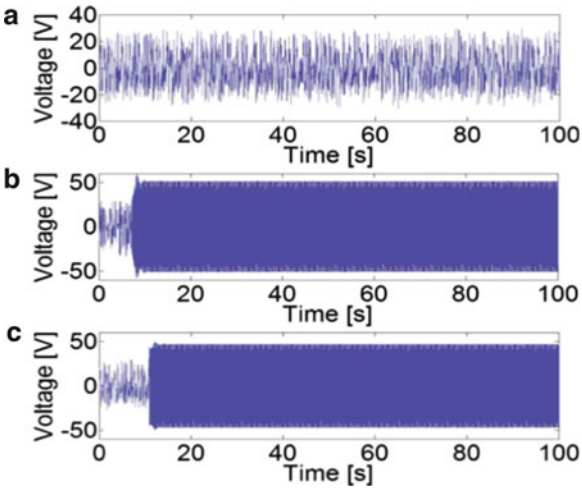

Fig. 2.35 Experimental voltage histories: (**a**) Chaotic strange attractor motion (excitation: $0.5 \times g$ at 8 Hz); (**b**) Large-amplitude periodic motion due to the excitation amplitude (excitation: $0.8 \times g$ at 8 Hz); (**c**) Large-amplitude periodic motion due to a disturbance at $t = 11\ s$ (excitation: $0.5 \times g$ at 8 Hz) ([53], copyright: American Institute of Physics)

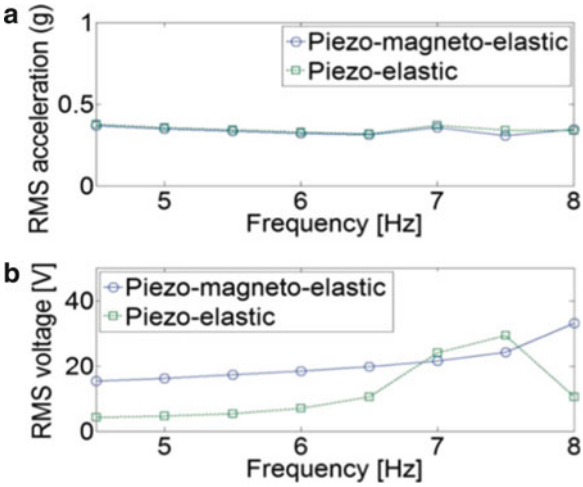

Fig. 2.36 (**a**) Root-mean-square (RMS) acceleration input at different frequencies (average value: $0.35 \times g$); (**b**) Open-circuit RMS voltage output over a wide frequency range ([53], copyright: American Institute of Physics)

initial deflection at one of the stable equilibriums, the voltage response could be chaotic strange attractor motion or large-amplitude periodic motion (limit cycle oscillation), under small or large harmonic excitations, as shown in Fig. 2.35a,b. The large-amplitude periodic motion could also be obtained under small excitation level by applying a disturbance or equivalently an initial velocity condition, as shown in Fig. 2.35c. Thus a large-amplitude response could be obtained at *off-resonance* frequencies as well as broadband performance, with a clear advantage over the linear piezoelastic configuration (with two magnets removed), as shown in Fig. 2.36. However, for small excitation amplitude, actuation energy is required to perturb the beam and hence drive the system into high-energy orbits, which was not addressed.

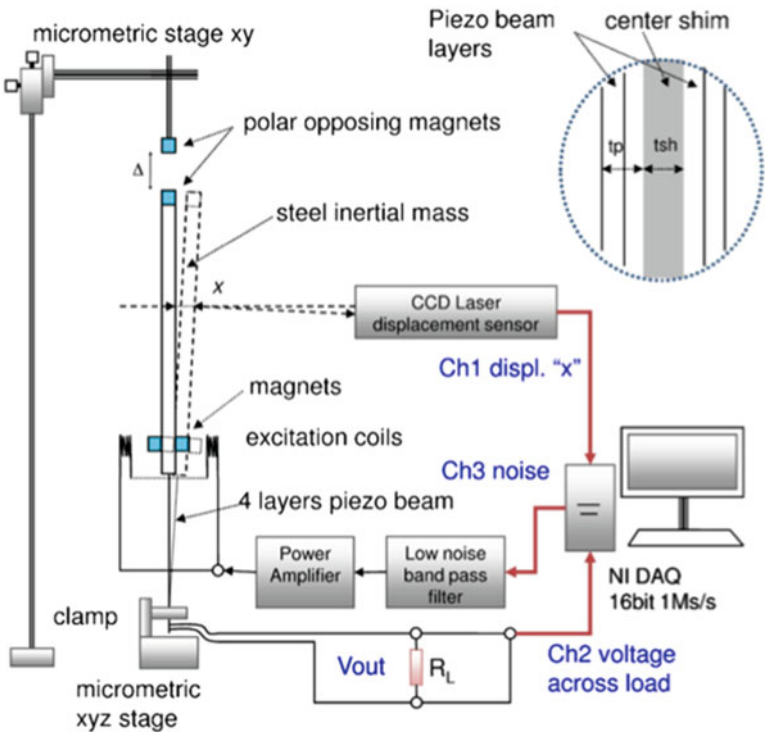

Fig. 2.37 Schematic of the experimental apparatus ([61], copyright: American Physical Society)

2.4.2.2 Stochastic Forcing

For a bistable system, stochastic forcing can also induce transitions between the stable equilibria of the system, and thus causing large-amplitude oscillations. Cottone et al. [61] realized a piezoelectric inverted pendulum by using the bistable mechanism (polar opposing magnets with a small separation distance Δ). Figure 2.37 shows the schematic of their experimental apparatus. The random vibration made the pendulum swing with small oscillations around each equilibrium or with large excursions from one equilibrium position to another. However, for extremely small Δ, the pronounced potential energy barrier confined the pendulum swing within one potential well. For specific Δ and noise level, the deflection of the pendulum x_{RMS} reached a maximum and hence the maximum power could exceed 4–6 times the power obtained when the magnets were far away (quasi-linear), as shown in Fig. 2.38.

Ferrari et al. [69], Lin and Alphenaar [70], Andò et al. [71], and Stanton et al. [52] extended this idea to study the energy harvesting performance of bistable cantilevers with repulsive magnets under wide-spectrum vibrations. From these studies, the critical issue for the broadband energy harvesting involves how to enable

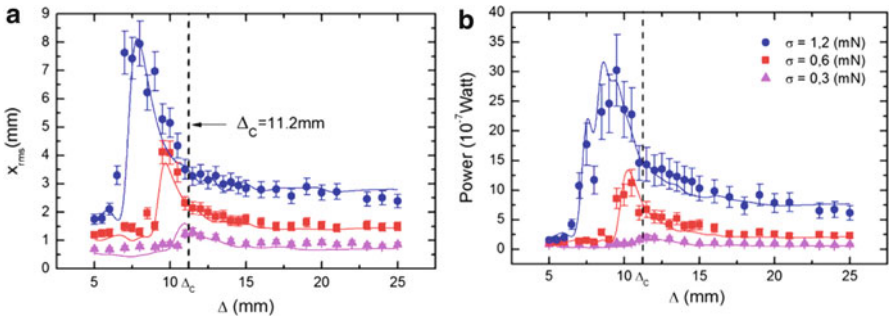

Fig. 2.38 (**a**) Position x_{RMS} and (**b**) power versus Δ for three different noise levels ([61], copyright: American Physical Society)

the harvester to readily transit between the two stable states, which is dependent on the excitation amplitude, frequency, and the extent of nonlinearity. For the bistable pendulum and a more general bistable dynamic system, Cottone et al. [61] concluded that (1) the raising of the response x_{RMS} is mainly due to the growth of the separation between the two minima of the potential function and (2) the drop of x_{RMS} is mainly due to the decrease in the jump probability caused by the increase of the potential barrier height δ (Fig. 2.26).

In order to increase the probability of transition between the potential wells and thus to further enhance the performance of a bistable system, some researchers [72, 73] have proposed to exploit the phenomenon of stochastic resonance. Stochastic resonance can occur if the dynamics of the system is forced such that the potential barrier oscillates, and this forcing matches with the mean time between transitions—i.e. the inverse Kramer's rate [74]. For a beam clamped at both ends, the SDOF bistable model is shown in Fig. 2.39. This is similar to the *snap-through* setup by Ramlan et al. [49], except that the distance A–A' between boundaries can be modulated at frequency ω and hence the potential barrier is modulated. Thus the parametrically forced dynamics of the system is defined as [72]

$$\ddot{\xi} + c\dot{\xi} - \mu\left(1 - \eta\cos\left(\omega t\right)\right)\xi + \xi^3 = Q(t), \tag{2.10}$$

where ξ is the nondimensional coordinate; c is the damping coefficient; μ is a measure of the compressive load acting on the beam; η and ω are the magnitude and frequency of forcing for modulation, respectively; and $Q(t)$ is the external noise. With this model, McInnes et al. [72] demonstrated that the properly tuned system in stochastic resonance by forcing (i.e., the forcing matched with inverse Kramer's rate) apparently experienced larger amplitude vibrations than those of the unforced mechanism, which was confined in a single potential well, as shown in Fig. 2.40. Thus, significantly more energy could be obtained. However, if the system was untuned, the net energy generated by the forcing mechanism could be less than the unforced mechanism, due to the energy consumed to force the boundaries to oscillate.

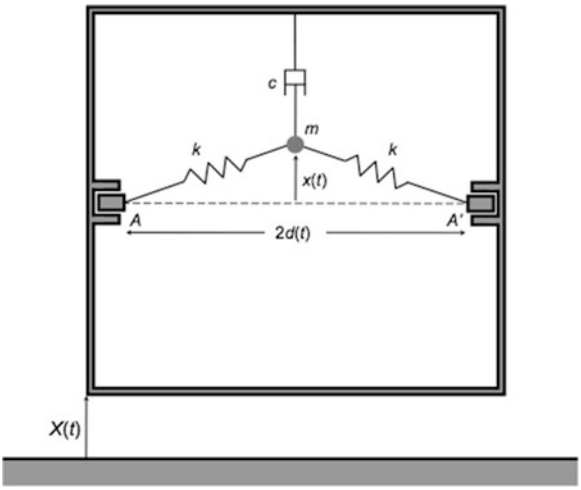

Fig. 2.39 One degree-of-freedom beam model, in which the distance A–A' can be modulated at frequency ω ([72], copyright: Elsevier)

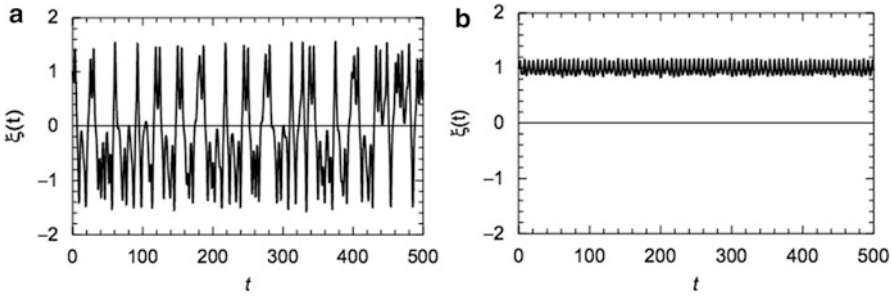

Fig. 2.40 Tuned system in stochastic resonance with $\omega = 1.2$: (**a**) response with forcing $\eta = 0.7$ and (**b**) response without forcing $\eta = 0$ ([72], copyright: Elsevier)

2.4.3 Configuration with Mechanical Stoppers

Piecewise-linear stiffness is another type of nonlinearity which can be introduced by mechanical stoppers. Soliman et al. [63] presented a micro-electromagnetic harvester incorporating such a mechanism, as shown in Fig. 2.27a. They investigated the benefit of such an architecture using mechanical stoppers via analytical, numerical, and experimental studies. They found that the new architecture increased the bandwidth of the harvester during a frequency upsweep, while maintaining the same bandwidth in a downsweep, as shown in Fig. 2.41. Similar to the Duffing-type hardening configuration, jump phenomenon and multiple solutions were observed during the frequency upsweep. They further investigated the benefit of stopper when the vibration frequency randomly changed in a range of 13.8 Hz centered around the natural frequency. In their numerical simulation, the harvester with one-sided stopper collected energy at a lower power level but for a larger fraction of time (due to a larger bandwidth), resulting in 30% more overall collected energy (Fig. 2.42).

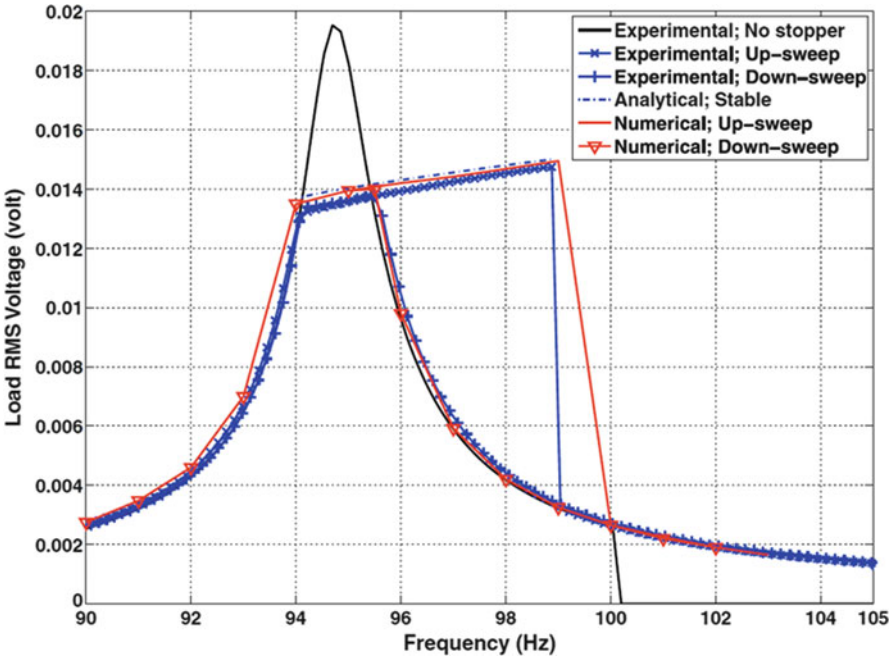

Fig. 2.41 Analytical, numerical, and experimental frequency responses of RMS load voltage from harvester with and without stopper ([63], copyright: IOP Publishing)

Blystad and Halvorsen [65] reported an experimental study on a piezoelectric harvester with a one-sided mechanical stopper under broadband vibrations. This device had a similar trend under sinusoidal sweep vibrations as in Soliman et al. [63]. Under colored noise vibrations, although wider bandwidth was achieved when the stopper became effective as the excitation level increased, the power output was smaller than the harvester without stopper (Fig. 2.43).

With increased bandwidth but lowered power level, the advantage of the harvester with stoppers is questionable. Soliman et al. [56] presented an optimization procedure for a harvester with stopper. They found that the performance of such a device is dominated by two factors: the stiffness ratio (k_2/k_1, refer to Fig. 2.27b) and the velocity of the beam at the impact point. These factors are controlled by the stopper height h_0 and the offset distance l_0 of the stopper from the cantilever support. Thus, in an environment with a known vibration probability density function (PDF), l_0 and h_0 should be tuned to tailor the upsweep bandwidth to better fit the given PDF, while h_0 should be set as high as possible to minimize contact damping and maximize energy collection.

Blystad et al. [64] presented circuit simulations to further investigate the effects of different two-sided stopper models and various interface circuits on the piezoelectric energy harvesting performance. Under harmonic excitations, they found that the output power was nearly unaffected by the stopper model used (elastic, critically damped, and completely inelastic stopper models). However, the

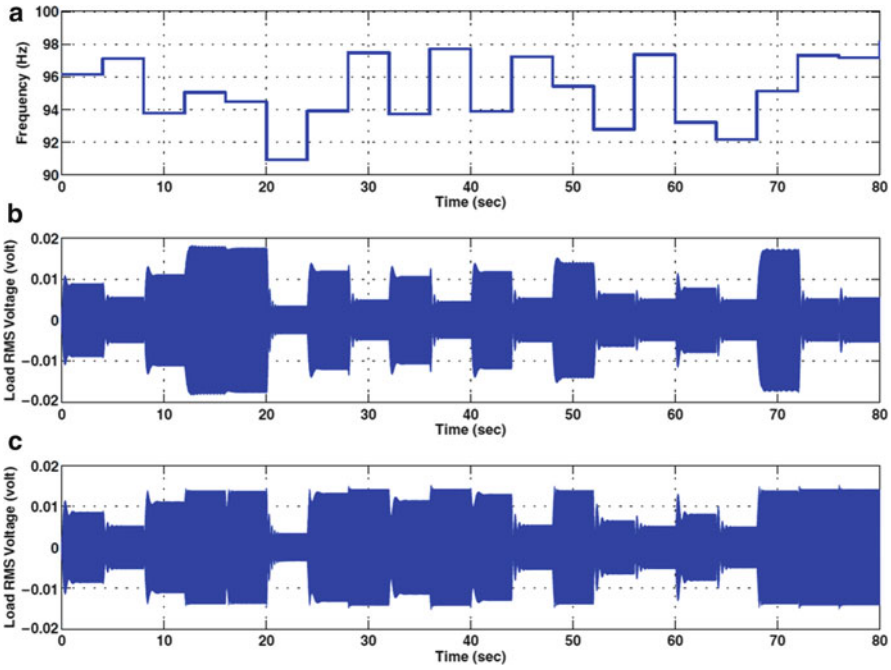

Fig. 2.42 (**a**) Time history of base excitation frequency and (**b**) RMS load voltage of no-stopper and (**c**) one-sided stopper harvesters by numerical simulation ([63], copyright: IOP Publishing)

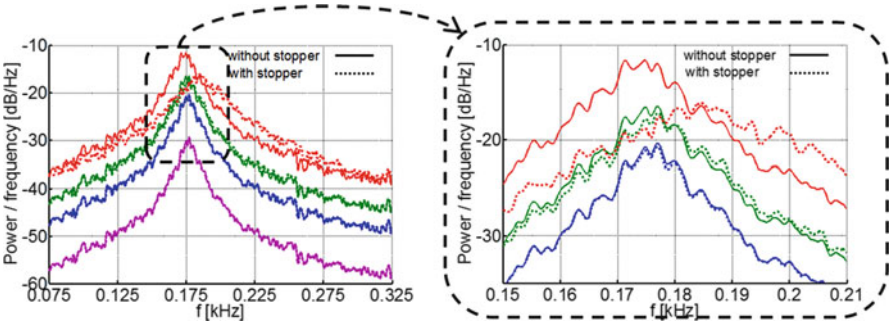

Fig. 2.43 Power spectral density of energy harvester output for increasing spectral density of excitation signal S_a. Without end stop (*solid line*) and with end stop (*dashed line*). $S_a = 0.087$, 0.82, 2.3, $8.0 \times 10^{-4} g^2 \mathrm{Hz}^{-1}$ starting from the lowest curve ([65], copyright: IOP Publishing)

stopper implementation did affect the jump phenomenon and thus the bandwidth during frequency upsweep. As to the different interface circuits, at low-excitation level (stopper not in effect), the sophisticated interfaces SECE and SSHI did not significantly enhance the performance. This is because the system they modeled

was not weakly coupled. Similar result can be found in Tang and Yang [75]. At high excitation level, the SECE and SSHI interfaces were found to lead to much better performance, especially for SSHI. This is because when the stopper becomes effective, the dynamics of the harvester is controlled by the stopper and less affected by piezoelectric coupling. Thus the system can be regarded as weakly coupled, for which case SECE and SSHI have been proved to be capable of enhancing system performance [75, 76]. Under random excitations, Blystad et al. [64] found that the damping in the stopper model significantly affected the output power, which is different from the harmonic excitation case. Furthermore, they found that SECE gave significant larger output power than the standard interface at large random excitation levels (i.e. frequent impacts with the stopper). Moreover, less power for large excitation level was observed as compared to the no-stopper configuration. This was consistent with the findings in Soliman et al. [56, 63] and in their experimental work [65] mentioned before.

2.4.4 Comments on Nonlinear Energy Harvesting Configuration

This section concentrates on exploiting the nonlinearity of a system for broadband energy harvesting, with a focus on nonlinear stiffness. The nonlinear energy harvester can be a Duffing-type oscillator with cubic nonlinear stiffness typically introduced by using magnets. It can also be a piecewise-linear oscillator with nonlinearity caused by a mechanical stopper.

- *Monostable nonlinear configuration.* In both hardening and softening monostable configurations, the resonance curve can be bent to the right or left when the nonlinearity is engaged. When the nonlinearity is sufficiently strong, a broad bandwidth energy harvesting could be achieved. The advantage imparted by the nonlinearity depends on the implementation of high-energy attractor. A linearly decreasing or increasing frequency sweep for the softening or hardening case respectively can capture the high-energy attractor motion and hence acquire a large-amplitude response over a wide bandwidth. However, such characteristics limit its practical application, i.e., the monostable energy harvester can only work in the condition that a slow and proper frequency sweep excitation exists. Besides, since multi-value and jump phenomenon near resonance occur with increased nonlinearity (Figs. 2.29c and 2.31), a mechanism should be implemented to perturb and drive the system into high-energy orbits in case the system vibrates in a low-energy branch. Otherwise the harvester provides much lower output power.
- *Bistable nonlinear configuration.* For a bistable system, large-amplitude oscillation can occur under both periodic and stochastic forcing. Under high-level periodic forcing or low-level forcing with proper perturbation, the bistable harvester can be driven into high-energy orbits. Hence, it can outperform the linear device over a wide bandwidth. Under stochastic forcing, the bistable

system also shows significant performance improvement when the system parameters are properly selected, such as the distance between magnets (Δ in Cottone et al. [61]). The performance of the bistable harvester can be further improved by exploiting the stochastic resonance, in which the boundary should be properly forced to periodically change the potential barrier height and hence the probability of the large-amplitude transition between the two stable states. However, actively achieving this by using actuators in such methods require external energy input and are quite difficult to implement.

- *Configuration with mechanical stoppers.* Under harmonic excitation, incorporating mechanical stoppers increases the bandwidth of the harvester during a frequency upsweep, while maintaining the same bandwidth in a downsweep. With the consideration of the lowered power level, the harvester with stopper during a downsweep definitely provides worse performance as compared to the harvester without stopper. Under random excitation, the performance of the harvester with stopper is controlled by the stopper height h_0 and the offset distance l_0 of the stopper from the cantilever support. Thus, in an environment with a known vibration probability density function (PDF), l_0 and h_0 should be tuned to tailor the upsweep bandwidth to better fit the given PDF and h_0 should be set as high as possible to minimize the contact damping and to maximize energy collection. Thus, it is possible to have better performance with a stopper in harmonic upsweep and random scenarios if the enlarged bandwidth can be tuned properly to have more significant influence on the overall harvested energy than the influence by the lowered power level. However, harvesters with mechanical stoppers may suffer from noise, fatigue, and mechanical wear.

2.5 Conclusions

The fundamental drawback of linear resonating harvesters, i.e., the narrow bandwidth, limits their application in practical scenarios where the ambient vibration source is frequency-variant or random. This chapter summarized recent advances in broadband energy harvesting techniques, including resonance tuning techniques, multimodal energy harvesting, and nonlinear techniques. Obviously, there are some other broadband techniques that cannot be categorized into the three groups described in this chapter, for example, the frequency up-conversion technique by magnetic excitation [77] and the optimal inductor technique of Renno et al. [78] (the optimal inductance level may not be practical and synthetic inductors are required).

Thus there appears to be no "one-fits all" broadband energy harvesting solution. Each technique reviewed in this chapter is only preferable in specific conditions. A suitable technique for broadband vibration energy harvesting should be selected according to the type of excitation (periodic or stochastic), the variation of frequency (infrequent or frequent), the excitation level and the targeted frequency range, etc. The merits, weakness, and applicability of current techniques are summarized in Table 2.2, it provides some guidance for developing vibration-based energy

Table 2.2 Merits, weakness, and applicability of various broadband energy harvesting techniques

Methods		Merits, weakness, and applicability
Resonant frequency tuning	Active tuning	• Usually implemented by piezoelectric methods • Limited tunability • Piezoceramic leakage aggravates tuning power consumption • Net power increase is achievable in limited range • Easy to implement automatic and continuous tuning during operation • Applicable when excitation frequency varies frequently or for random excitation in a limited range, given affordable tuning power consumption
	Passive tuning	• Mostly by mechanical and magnetic methods • Relatively large tunability • For manual tuning or using controller for self-tuning: (i) Large power consumption for actuation (ii) Difficult to implement self-powered automatic control system for tuning (iii) Applicable when excitation frequency varies infrequently (iv) Complexity in system design and integration, especially for magnetic methods • Some exceptions in mechanical methods using inertia force: (i) Totally passive (no need of external tuning power) (ii) Self-adaptive to excitation frequency (iii) Continuous tuning during operation (iv) Applicable for specific conditions (e.g., rotational motion)
Multimodal energy harvesting		• Much easier to implement than resonance tuning techniques • Exploits multiple bending modes of a continuous beam or a cantilever array configuration • For a continuous beam, usually only first two modes contribute to effective energy harvesting • For a cantilever array configuration, continuous and larger bandwidth can be achieved but with significant sacrifice of power density • Should be designed with proper parameters to cover the targeted frequency range with least sacrifice of power density • Requires complex interface circuit to avoid voltage cancelation
Nonlinear techniques	Monostable	• Applicable for excitations with slow and proper frequency sweep • Requires certain perturbation when the harvester enters low-energy orbits
	Bistable	• Applicable for high-level periodic excitation • Applicable for low-level periodic excitation but with certain perturbation mechanism to drive the harvester into high-energy orbits • Applicable for random excitation with properly designed potential barrier at given excitation level • Further performance enhancement achievable by using stochastic resonance, which requires proper actuation and extra power
	Mechanical stopper	• Increases bandwidth by frequency upsweep • Increases bandwidth under random excitation with properly selected stopper parameters • Lowered power level • Modest performance improvement with enlarged bandwidth when tuned to fit a given vibration spectrum and thus to have a more significant influence on overall harvested energy • Suffers from noise, fatigue, and mechanical wear

harvesters. It is envisioned that, with further improvement of these broadband techniques, the concept of vibration energy harvesting will approach practical deployment in industrial applications as well as in our daily life.

References

1. Roundy S, Wright PK, Rabaey J (2003) A study of low level vibrations as a power source for wireless sensor nodes. Comput Commun 26:1131–1144
2. Mitcheson PD, Green TC, Yeatman EM, Holmes AS (2004) Architectures for vibration-driven micropower generators. J Microelectromech Syst 13:429–440
3. El-Hami M, Glynne-Jones P, White NM, Beeby S, James E, Brown AD, Ross JN (2001) Design and fabrication of a new vibration-based electromechanical power generator. Sens Actuators A 92:335–342
4. Anton SR, Sodano HA (2007) A review of power harvesting using piezoelectric materials (2003–2006). Smart Mater Struct 16:R1–R21
5. Yang YW, Tang LH, Li HY (2009) Vibration energy harvesting using macro-fiber composites. Smart Mater Struct 18:115025
6. Erturk A, Inman DJ (2008) A distributed parameter electromechanical model for cantilevered piezoelectric energy harvesters. J Vib Acoust 130:041002
7. De Marqui C Jr, Erturk A, Inman DJ (2009) An electromechanical finite element model for piezoelectric energy harvester plates. J Sound Vib 327:9–25
8. Yang YW, Tang LH (2009) Equivalent circuit modeling of piezoelectric energy harvesters. J Intell Mater Syst Struct 20:2223–2235
9. Elvin NG, Elvin AA (2009) A general equivalent circuit model for piezoelectric generators. J Intell Mater Syst Struct 20:3–9
10. Roundy S, Zhang Y (2005) Toward self-tuning adaptive vibration based micro-generators. Proc SPIE 5649:373–384
11. Leland ES, Wright PK (2006) Resonance tuning of piezoelectric vibration energy scavenging generators using compressive axial preload. Smart Mater Struct 15:1413–1420
12. Eichhorn C, Goldschmidtboeing F, Woias P (2008) A frequency tunable piezoelectric energy converter based on a cantilever beam. In: Proceedings of PowerMEMS, pp 309–312
13. Hu Y, Xue H, Hu H (2007) A piezoelectric power harvester with adjustable frequency through axial preloads. Smart Mater Struct 16:1961–1966
14. Morris DJ, Youngsman JM, Anderson MJ, Bahr DF (2008) A resonant frequency tunable, extensional mode piezoelectric vibration harvesting mechanism. Smart Mater Struct 17:065021
15. Youngsman JM, Luedeman T, Morris DJ, Andersonb MJ (2010) A model for an extensional mode resonator used as a frequency-adjustable vibration energy harvester. J Sound Vib 329:277–288
16. Loverich J, Geiger R, Frank J (2008) Stiffness nonlinearity as a means for resonance frequency tuning and enhancing mechanical robustness of vibration power harvesters. Proc SPIE 6928:692805
17. Wu X, Lin J, Kato S, Zhang K, Ren T, Liu L (2008) A frequency adjustable vibration energy harvester. In: Proceedings of PowerMEMS, pp 245–248
18. Gu L, Livermore C (2010) Passive self-tuning energy harvester for extracting energy from rotational motion. Appl Phys Lett 97:081904
19. Jo SE, Kim MS, Kim YJ (2011) Passive-self-tunable vibrational energy harvester. In: Proceedings of 16th international solid-state sensors, actuators and microsystems conference (TRANSDUCERS), pp 691–694
20. Challa VR, Prasad MG, Shi Y, Fisher FT (2008) A vibration energy harvesting device with bidirectional resonance frequency tunability. Smart Mater Struct 17:015035

21. Reissman T, Wolff EM, Garcia E (2009) Piezoelectric resonance shifting using tunable nonlinear stiffness. Proc SPIE 7288:72880G
22. Zhu D, Roberts S, Tudor J, Beeby S (2008) Closed loop frequency tunning of A vibration-based microgenerator. In: Proceedings of PowerMEMS, pp 229–232
23. Ayala-Garcia IN, Zhu D, Tudor MJ, Beeby SP (2010) A tunable kinetic energy harvester with dynamic over range protection. Smart Mater Struct 19:115005
24. Challa VR, Prasad MG, Fisher FT (2011) Towards an autonomous self-tuning vibration energy harvesting device for wireless sensor network applications. Smart Mater Struct 20:025004
25. Wu W, Chen Y, Lee B, He J, Peng Y (2006) Tunable resonant frequency power harvesting devices. Proc SPIE 6169:61690A
26. Peters C, Maurath D, Schock W, Mezger F, Manoli Y (2009) A closed-loop wide-range tunable mechanical resonator for energy harvesting systems. J Micromech Microeng 19:094004
27. Lallart M, Anton SR, Inman DJ (2010) Frequency self-tuning scheme for broadband vibration energy harvesting. J Intell Mater Syst Struct 21:897–906
28. Zhu D, Tudor J, Beeby S (2010) Strategies for increasing the operating frequency range of vibration energy harvesters: a review. Meas Sci Technol 21:022001
29. Wischke M, Masur M, Goldschmidtboeing F, Woias P (2010) Electromagnetic vibration harvester with piezoelectrically tunable resonance frequency. J Micromech Microeng 20:035025
30. Jang S-J, Rustighi E, Brennan MJ, Lee YP, Jung H-J (2011) Design of a 2DOF vibrational energy harvesting device. J Intell Mater Syst Struct 22:443–448
31. Aldraihem O, Baz A (2011) Energy harvester with a dynamic magnifier. J Intell Mater Syst Struct 22:521–530
32. Tang X, Zuo L (2011) Enhanced vibration energy harvesting using dual-mass systems. J Sound Vib 330:5199–5209
33. Roundy S, Leland ES, Baker J, Carleton E, Reilly E, Lai E, Otis B, Rabaey JM, Wright PK, Sundararajan V (2005) Improving power output for vibration-based energy scavengers. IEEE Pervasive Comput 4:28–36
34. Yang B, Lee C, Xiang W, Xie J, He JH, Krishna Kotlanka R, Low SP, Feng H (2009) Electromagnetic energy harvesting from vibrations of multiple frequencies. J Micromech Microeng 19:035001
35. Tadesse Y, Zhang S, Priya S (2009) Multimodal energy harvesting system: piezoelectric and electromagnetic. J Intell Mater Syst Struct 20:625–632
36. Ou Q, Chen X, Gutschmidt S, Wood A, Leigh N (2010) A two-mass cantilever beam model for vibration energy harvesting applications. In: Proceedings of 6th annual IEEE conference on automation science and engineering (CASE), pp 301–306
37. Arafa M, Akl W, Aladwani A, Aldrarihem O, Baz A (2011) Experimental implementation of a cantilevered piezoelectric energy harvester with a dynamic magnifier. Proc SPIE 7977:79770Q
38. Erturk A, Renno JM, Inman DJ (2009) Modeling of piezoelectric energy harvesting from an L-shaped beam-mass structure with an application to UAVs. J Intell Mater Syst Struct 20: 529–544
39. Berdy DF, Jung B, Rhoads JF, Peroulis D (2011) Increased-bandwidth, meandering vibration energy harvester. In: Proceedings of 16th international solid-state sensors, actuators and microsystems conference (TRANSDUCERS), pp 2638–2641
40. Wu H, Tang LH, Yang YW, Soh CK (2011) A novel 2-DOF piezoelectric energy harvester. 22nd international conference on adaptive structures and technologies (ICAST), Corfu, Greece, 10–12 October, paper no. 077
41. Yang Z, Yang J (2009) Connected vibrating piezoelectric bimorph beams as a wide-band piezoelectric power harvester. J Intell Mater Syst Struct 20:569–574
42. Kim I-H, Jung H-J, Lee BM, Jang S-J (2011) Broadband energy-harvesting using a two degree-of-freedom vibrating body. Appl Phys Lett 98:214102
43. Shahruz SM (2006) Design of mechanical band-pass filters for energy scavenging. J Sound Vib 292:987–998
44. Xue H, Hu Y, Wang Q (2008) Broadband piezoelectric energy harvesting devices using multiple bimorphs with different operating frequencies. IEEE Trans Ultrason Ferroelectr Freq Control 55:2104–2108

45. Ferrari M, Ferrari V, Guizzetti M, Marioli D, Taroni A (2008) Piezoelectric multifrequency energy converter for power harvesting in autonomous microsystems. Sens Actuators A 142:329–335
46. Liu J, Fang H, Xu Z, Mao X, Shen X, Chen D, Liao H, Cai B (2008) A MEMS-based piezoelectric power generator array for vibration energy harvesting. Microelectron J 39: 802–806
47. Sari I, Balkan T, Kulah H (2008) An electromagnetic micro power generator for wideband environmental vibrations. Sens Actuatators A 145–146:405–413
48. Cheng S, Jin Y, Rao Y, Arnold DP (2009) A bridge voltage doubler AC/DC converter for low-voltage energy harvesting applications. In: Proceedings of PowerMEMS, pp 25–28
49. Ramlan R, Brennan MJ, Mace BR, Kovacic I (2010) Potential benefits of a non-linear stiffness in an energy harvesting device. Nonlinear Dyn 59:545–558
50. Mann BP, Sims ND (2009) Energy harvesting from the nonlinear oscillations of magnetic levitation. J Sound Vib 319:515–530
51. Stanton SC, McGehee CC, Mann BP (2009) Reversible hysteresis for broadband magnetopiezoelastic energy harvesting. Appl Phys Lett 95:174103
52. Stanton SC, McGehee CC, Mann BP (2010) Nonlinear dynamics for broadband energy harvesting: investigation of a bistable piezoelectric inertial generator. Physica D 239:640–653
53. Erturk A, Hoffmann J, Inman DJ (2009) A piezomagnetoelastic structure for broadband vibration energy harvesting. Appl Phys Lett 94:254102
54. Marinkovic B, Koser H (2009) Smart sand—a wide bandwidth vibration energy harvesting platform. Appl Phys Lett 94:103505
55. Hajati A, Kim S-G (2011) Ultra-wide bandwidth piezoelectric energy harvesting. Appl Phys Lett 99:083105
56. Soliman MSM, Abdel-Rahman EM, El-Saadany EF, Mansour RR (2009) A design procedure for wideband micropower generators. J Microelectromech Syst 18:1288–1299
57. Lin J, Lee B, Alphenaar B (2010) The magnetic coupling of a piezoelectric cantilever for enhanced energy harvesting efficiency. Smart Mater Struct 19:045012
58. Triplett A, Quinn DD (2009) The effect of non-linear piezoelectric coupling on vibration-based energy harvesting. J Intell Mater Syst Struct 20:1959–1967
59. Stanton SC, Erturk A, Mann BP, Inman DJ (2010) Nonlinear piezoelectricity in electroelastic energy harvesters: modeling and experimental identification. J Appl Phys 108:074903
60. Erturk A, Inman DJ (2008) Issues in mathematical modeling of piezoelectric energy harvesters. Smart Mater Struct 17:065016
61. Cottone F, Vocca H, Gammaitoni L (2009) Nonlinear energy harvesting. Phys Rev Lett 102:080601
62. Gammaitoni L, Neri I, Vocca H (2009) Nonlinear oscillators for vibration energy harvesting. Appl Phys Lett 94:164102
63. Soliman MSM, Abdel-Rahman EM, El-Saadany EF, Mansour RR (2008) A wideband vibration-based energy harvester. J Micromech Microeng 18:115021
64. Blystad L-CJ, Halvorsen E, Husa S (2010) Piezoelectric MEMS energy harvesting systems driven by harmonic and random vibrations. IEEE Trans Ultrason Ferroelectr Freq Control 57:908–919
65. Blystad L-CJ, Halvorsen E (2011) An energy harvester driven by colored noise. Smart Mater Struct 20:025011
66. Moehlis J, DeMartini BE, Rogers JL, Turner KL (2009) Exploiting nonlinearity to provide broadband energy harvesting. In: Proceedings of ASME dynamic systems and control conference, DSCC2009-2542
67. Daqaq MF (2010) Response of uni-modal Duffing-type harvesters to random forced excitations. J Sound Vib 329:3621–3631
68. Erturk A, Inman DJ (2011) Broadband piezoelectric power generation on high-energy orbits of the bistable Duffing oscillator with electromechanical coupling. J Sound Vib 330:2339–2353
69. Ferrari M, Ferrari V, Guizzetti M, Andò B, Baglio S, Trigona C (2010) Improved energy harvesting from wideband vibrations by nonlinear piezoelectric converters. Sens Actuators A 162:425–431

70. Lin J, Alphenaar B (2010) Enhancement of energy harvested from a random vibration source by magnetic coupling of a piezoelectric cantilever. J Intell Mater Syst Struct 21:1337–1341
71. Andò B, Baglio S, Trigona C, Dumas N, Latorre L, Nouet P (2010) Nonlinear mechanism in MEMS devices for energy harvesting applications. J Micromech Microeng 20:125020
72. McInnes CR, Gorman DG, Cartmell MP (2008) Enhanced vibrational energy harvesting using nonlinear stochastic resonance. J Sound Vib 318:655–662
73. Formosa F, Büssing T, Badel A, Marteau S (2009) Energy harvesting device with enlarged frequency bandwidth based on stochastic resonance. In: Proceedings of PowerMEMS, pp 229–232
74. Wellens T, Shatokhin V, Buchleitner A (2004) Stochastic resonance. Rep Prog Phys 67:45–105
75. Tang LH, Yang YW (2011) Analysis of synchronized charge extraction for piezoelectric energy harvesting. Smart Mater Struct 20:085022
76. Shu YC, Lien IC, Wu WJ (2007) An improved analysis of the SSHI interface in piezoelectric energy harvesting. Smart Mater Struct 16:2253–2264
77. Wickenheiser AM, Garcia E (2010) Broadband vibration-based energy harvesting improvement through frequency up-conversion by magnetic excitation. Smart Mater Struct 19:065020
78. Renno JM, Daqaq MF, Inman DJ (2009) On the optimal energy harvesting from a vibration source. J Sound Vib 320:386–405

http://www.springer.com/978-1-4614-5704-6

Advances in Energy Harvesting Methods

Elvin, N.; Erturk, A. (Eds.)
2013, X, 455 p., Hardcover
ISBN: 978-1-4614-5704-6